Review

Generative Models for Medical Image Creation and Translation: A Systematic Review

Haowen Pang , Tiande Zhang , Yanan Wu , Shannan Chen , Wei Qian , Yudong Yao , Chuyang Ye , Patrice Monkam * , Shouliang Qi *

Posted Date: 17 December 2025

doi: 10.20944/preprints202512.1407.v1

Keywords: generative model; medical image; generative adversarial networks; deep learning

Review

Generative Models for Medical Image Creation and Translation: A Systematic Review

Haowen Pang [1,2,†], Tiande Zhang [1,3,†], Yanan Wu [4], Shannan Chen [1,5], Wei Qian [1,5], Yudong Yao [6], Chuyang Ye [2], Patrice Monkam [1,5,*] and Shouliang Qi [1,5,*]

[1] College of Medicine and Biological Information Engineering, Northeastern University, Shenyang, China
[2] School of Integrated Circuits and Electronics, Beijing Institute of Technology, Beijing, China
[3] School of Computer Science and Technology, Harbin Institute of Technology, Harbin, China
[4] School of Health Management, China Medical University, Shenyang, China
[5] Key Laboratory of Intelligent Computing in Medical Image, Ministry of Education, Northeastern University, Shenyang, China
[6] Department of Electrical and Computer Engineering, Stevens Institute of Technology, Hoboken, USA
* Correspondence: patrice123china1@gmail.com (P.M.); qisl@bmie.neu.edu.cn (S.Q.); Tel.: +86-24-8368-0230; Fax: +86-24-8368-1955
† These authors contributed equally to this work.

Abstract

Generative models play a pivotal role in the field of medical imaging. This paper provides an extensive and scholarly review of the application of generative models in medical image creation and translation. In the creation aspect, the goal is to generate new images based on potential conditional variables, while in translation, the aim is to map images from one or more modalities to another, preserving semantic and informational content. The review begins with a thorough exploration of a diverse spectrum of generative models, including Variational Autoencoders (VAEs), Generative Adversarial Networks (GANs), Diffusion Models (DMs), and their respective variants. The paper then delves into an insightful analysis of the merits and demerits inherent to each model type. Subsequently, a comprehensive examination of tasks related to medical image creation and translation is undertaken. For the creation aspect, papers are classified based on downstream tasks such as image classification, segmentation, and others. In the translation facet, papers are classified according to the target modality. A chord diagram depicting medical image translation across modalities, including Magnetic Resonance Imaging (MRI), Computed Tomography (CT), Cone Beam CT (CBCT), X-ray radiography, Positron Emission Tomography (PET), and ultrasound imaging, is presented to illustrate the direction and relative quantity of previous studies. Additionally, the chord diagram of MRI image translation across contrast mechanisms is also provided. The final section offers a forward-looking perspective, outlining prospective avenues and implementation guidelines for future research endeavors.

Keywords: generative model; medical image; generative adversarial networks; deep learning

1. Background

In recent years, deep learning has gained widespread prominence in medical image analysis [1–7]. Within the scope of this review, we focus on one of the most compelling applications of deep learning: generative AI in medical imaging-a dynamic and rapidly advancing field of research. The rapid advancement of deep learning and computer vision over the past few decades has had profound implications across a wide range of applications, with the field of medical image generation significantly benefiting from these developments [8–14].

In this review, we focus on the application of generative models to medical image creation and modality translation. As shown in Figure 1, image creation aims to generate new images based on

 doi:10.20944/preprints202512.1407.v1

potential conditional variables. In deep learning-based image generation, a large dataset of real images is typically used to train the model initially. Subsequently, random noise or conditional inputs are utilized to produce new images. This approach is primarily employed to address challenges in medical imaging, such as data scarcity, insufficient annotations, and severe class imbalances, which are common obstacles in training robust deep learning models [15,16].

Imaging modalities, including Magnetic Resonance Imaging (MRI), Computed Tomography (CT), and Positron Emission Tomography (PET), are commonly used in clinical workflow, each providing unique structural, functional, and metabolic information [17]. Image translation aims to map images from one or more modalities to another while preserving semantic and informational content. The primary goal of medical image translation is to optimize clinical workflows, particularly in situations where traditional imaging methods are impractical due to constraints related to time, labor, or cost [18].

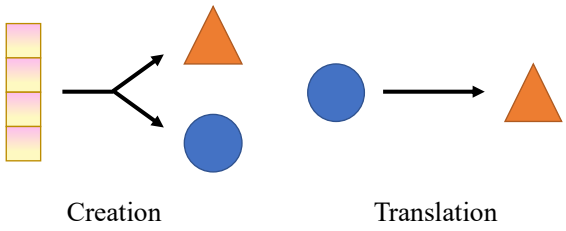

Figure 1. Creation and translation in medical image generation.

In this context, several key questions guide our investigation: What are the latest advancements in generative models for medical image creation and cross-modality translation? How do different generative model architectures—such as generative adversarial networks (GANs), variational autoencoders (VAEs), and diffusion models —perform in the context of medical imaging, and what are their respective strengths and limitations? Furthermore, how do advanced optimization strategies, including adversarial training, uncertainty modeling, and gradient perturbation, contribute to improving the fidelity, realism, and clinical utility of synthetic medical images? Finally, what are the primary evaluation metrics used to assess the quality, anatomical accuracy, and clinical applicability of these generated images, and how do these metrics align with the standards of real-world medical practice? By addressing these questions, this review aims to provide a comprehensive understanding of the current state of generative models in medical imaging, highlight emerging trends, and identify areas for future research that could further enhance the capabilities and clinical integration of these powerful technologies.

In this review, we categorize the relevant literature according to their respective applications and thoroughly examine their clinical implications. Furthermore, we explore recent trends and potential future directions in the field. To summarize, the primary contributions of our work are as follows:

1. This review conducts a thorough review of three widely employed generative models: VAEs, GANs, and diffusion models (DMs). We outline algorithms within these generative models that have found extensive applications in the domain of medical image analysis and provide analyses thereof.
2. This review categorizes the applications of generative models in medical image analysis into creation and translation. We present an extensive review of creation methods and classify their downstream applications into three distinct categories: classification, segmentation, and others. We classify translation methods based on the target modality.
3. This review organizes previous studies into categories and offer practical implementation guidelines gleaned from the lessons learned in these works.

The architecture of this review is shown in Figure 2. In Section 2, we provided a comprehensive comparison with related works. In Section 3, we introduced the search methods for literature and

 doi:10.20944/preprints202512.1407.v1

analyzed the trend of the generated model's publication. In Section 4, we introduced three most used generation models, VAEs, GANs, DMs, and their variants. In Section 5, we reviewed medical image creation and classified the literature according to different downstream tasks. In Section 6, we reviewed medical image translation and classified the literature according to different target modalities. In Section 7, we summarized the application of generative models in medical image creation and translation and provided implementation guidelines, as well as limitations and future research in this review.

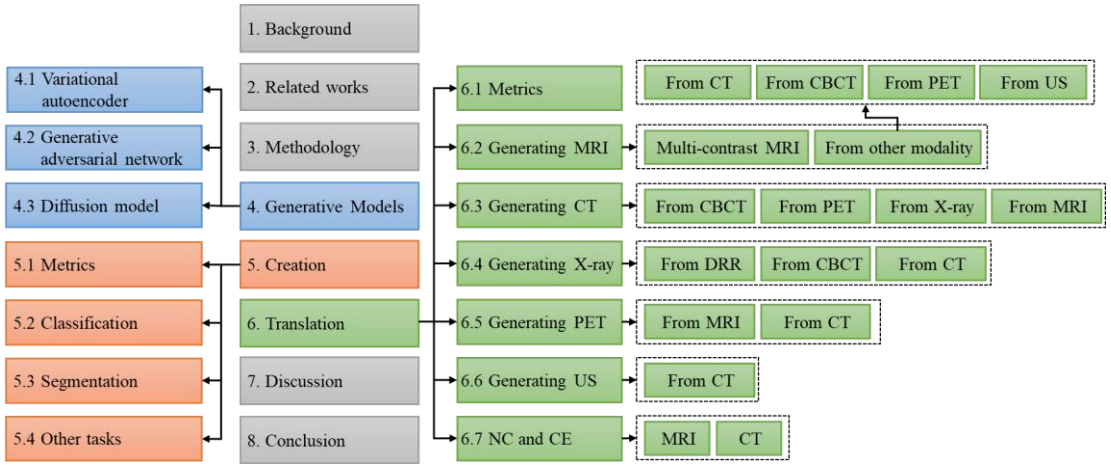

Figure 2. Section organization.

2. Related Works

Numerous studies have reviewed the application of generative models in medical image analysis, reflecting the rapid development and growing interest in this field. Yi et al. [19] conducted an early review of the applications of GANs in medical image analysis, covering research up to October 2018. Similar to the work of Yi et al., Kazeminia et al. [20] extended this work by reviewing the applications of GANs in medical image analysis up to October 2019. Their review comprehensively categorized the use of GANs across various tasks, including medical image synthesis, segmentation, reconstruction, detection, denoising, registration, and classification.

Beyond GAN-specific reviews, Wang et al. [18] provided a broader perspective by examining deep learning-based methods for medical image translation, highlighting advancements in cross-modality image synthesis. Dayarathna et al. [17] conducted a comprehensive survey on deep learning-based medical image translation, covering research from 2018 to 2023. Their review focused on the generation of pseudo-CT, synthetic MR, and synthetic PET images, providing a detailed overview of synthetic contrasts in medical imaging. Additionally, they summarized the most frequently employed deep learning architectures for medical image synthesis, highlighting key methodologies and their applications in cross-modality image generation.

Additionally, several studies have focused specifically on the role of GANs in medical image augmentation. Chen et al. [21], Goceri et al. [15], and Kebaili et al. [16] conducted a comprehensive and systematic review and analysis of GAN based medical image augmentation work. Osuala et al. [22] reviewed the application of image synthesis and adversarial networks in the field of cancer imaging. Zhao et al. [23] summarized the application of GAN based on attention mechanism in tasks such as medical image segmentation, synthesis, and detection.

While these reviews provide valuable insights into the use of GANs and related techniques across diverse medical imaging tasks, there remains a significant gap in the literature. To date, no comprehensive review focuses exclusively on the application of deep learning-based generative models for medical image creation and cross-modality translation. Given the increasing complexity of modern generative architectures—such as diffusion models, VAEs, and transformer-based models—and their transformative potential in medical imaging, a dedicated review in this area is

 doi:10.20944/preprints202512.1407.v1

both timely and necessary. This work aims to address this gap by systematically analyzing recent advancements in deep learning-based generative models for medical image synthesis and translation, with a focus on their clinical relevance, methodological innovations, and future research directions.

3. Methodology

We conducted a rigorous and comprehensive literature search across multiple well-established academic databases, including Web of Science, Google Scholar, Elsevier, Springer, and IEEE Xplore, to ensure the inclusion of high-quality and diverse studies on generative models for medical image creation and translation. Our search strategy was meticulously designed to capture a broad spectrum of relevant research while maintaining precision and relevance. We employed a combination of targeted keywords and phrases, such as "generative models," "medical image synthesis," "GAN," "diffusion models," and "image translation," using Boolean operators (e.g., AND, OR) to construct complex search queries that enhanced the sensitivity and specificity of the search. To maintain a contemporary focus, we restricted the search to peer-reviewed articles published between 2018 and 2023, thereby reflecting the latest advancements and emerging trends in the field. Preprint papers were deliberately excluded from our analysis due to the absence of rigorous peer-review processes, ensuring that only validated and credible research findings were considered.

The selection process was conducted in multiple stages to uphold methodological rigor and reduce potential bias. Initially, we performed a broad screening of article titles and abstracts to identify studies potentially meeting our inclusion criteria. This was followed by a comprehensive full-text review of shortlisted articles, which was independently performed by two authors. Studies were included if they explicitly applied generative models to medical image synthesis, provided detailed descriptions of model architectures and training methodologies, and quantitatively evaluated model performance using established metrics. We excluded articles that lacked methodological transparency, focused solely on theoretical aspects without empirical validation, or addressed non-medical applications. Any disagreements between the two reviewers were resolved through discussion, with unresolved discrepancies adjudicated by a third author to ensure consensus and objectivity. This multi-step screening approach minimized selection bias and enhanced the reliability and reproducibility of our study identification process.

In this review, we exclude the applications of generative models in medical image denoising, reconstruction, super-resolution, registration, etc. This review focuses on modalities primarily used for clinical diagnosis, such as CT, MRI, X-Ray, and PET. These modalities can non-invasively obtain images of entire organs or systems, aiding in clinical diagnosis and treatment monitoring. In this review, we exclude imaging modalities used for studying the microscopic structure of cells and tissues, such as histology and fluorescence microscopy. These modalities are common in pathology, cell biology, and molecular biology research, and are mainly used in laboratory settings to study features at the cellular and molecular levels. They rely on tissue sections and staining techniques, making them suitable for detailed observation at the cellular and tissue levels.

Through this meticulous and systematic screening, we identified a total of **232** articles that met all predefined inclusion criteria. These articles were incorporated into our review, providing a more extensive and structured analysis compared to prior surveys on the same topic [18,19,21,23,24]. Our systematic approach not only ensures comprehensive coverage of the literature but also facilitates a critical examination of the methodologies, optimization strategies, and clinical implications of generative models in medical imaging. To provide a clear visual representation of our search and selection process, Figure 3 presents a detailed flowchart outlining each stage, from the initial identification of studies to the final inclusion. This figure also illustrates the distribution of the selected articles across different model architectures and medical imaging applications, offering valuable insights into current research trends and gaps in the field.

 doi:10.20944/preprints202512.1407.v1

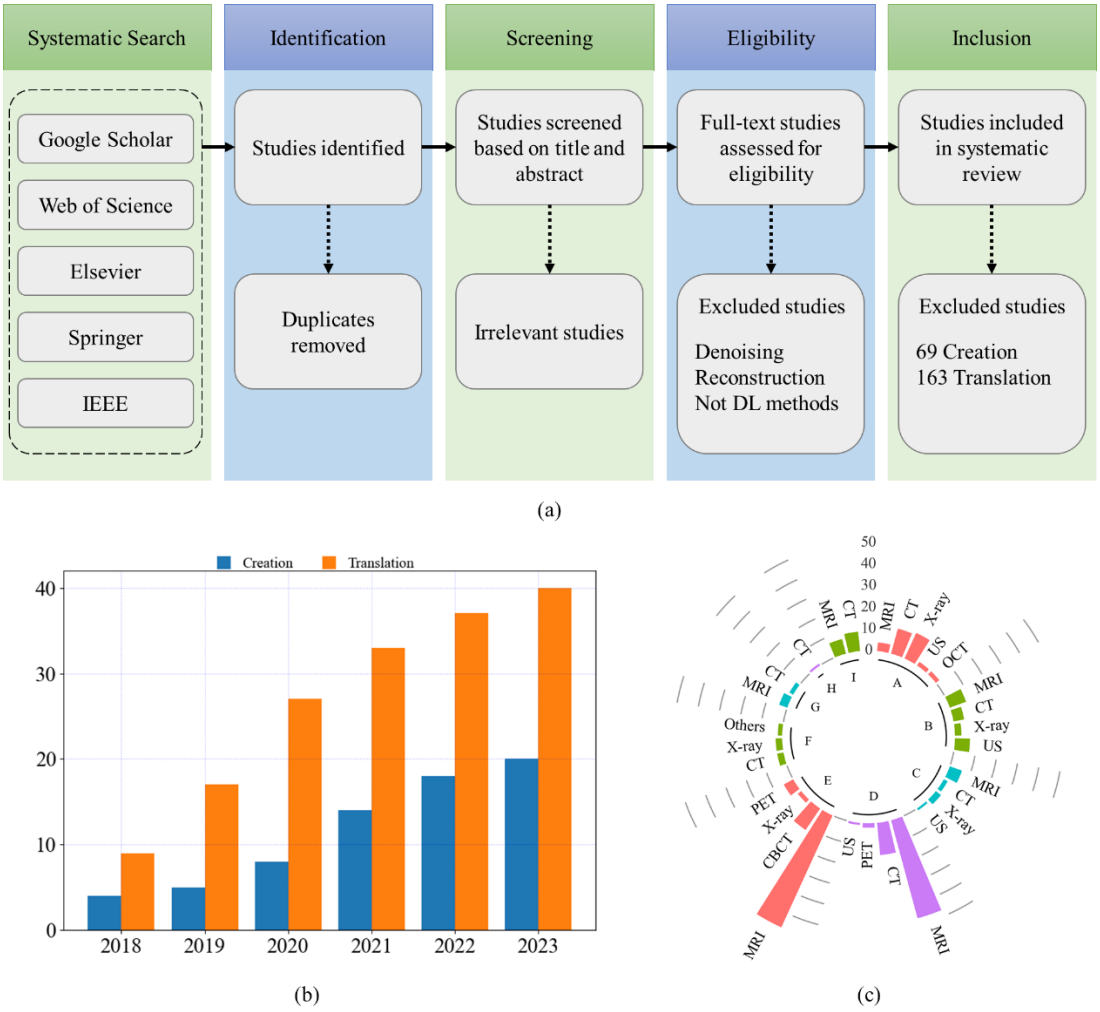

Figure 3. Literature search and analysis. (a) The PRISMA flowchart for this review. (b) The distribution of articles by year of publication. (c) The distribution of articles by task and modality. A: Creation for classification; B: Creation for segmentation; C: Creation for other tasks; D: Translate to MRI; E: Translate to CT; F: Translate to X-ray; G: Translate to PET; H: Translate to Ultrasound; I: Translation with Non- and Contrast Enhanced image.

4. Generative Models

Generative models are designed to learn the underlying distribution of a given dataset, in order to generate new data points that resemble the original dataset [25]. These models can generate new data samples that are like the training data, but not identical. Some popular generative models include VAE, GANs, and DMs.

4.1. Variational Autoencoder

VAEs [26] have already shown promise in generating complicated nature image [27–29] and medical image [30,31]. As show in Figure 4, the VAE model comprises an encoder network that transforms input data into a latent space representation and a decoder network that reconstructs new data samples from this latent space. Unlike conventional autoencoders, VAEs learn a probabilistic representation of the input data, enabling them to generate novel data samples that closely resemble the original input data [32]. VAEs can generate new, synthetic medical images that are similar to the original training data, which can be used to augment training datasets and improve the performance of machine learning models. However, the images generated by VAEs tend to be blurrier compared to those generated by other generative models like GANs. This is due to the inherent nature of the VAE's probabilistic framework, which averages over many possible outputs.

 doi:10.20944/preprints202512.1407.v1

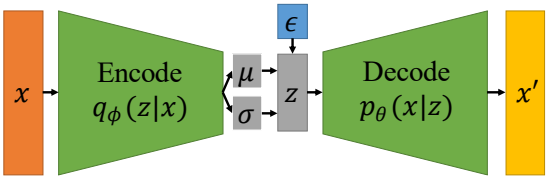

Figure 4. Architecture of VAE.

In Figure 4, x represents the input image, which is fed into the encoder to obtain two sets of encodings, namely the mean encoding μ and the variance encoding σ. ϵ represents the random noise encoding. By combining the original encoding with the noise encoding after weighted allocation, a new latent code z is obtained, which is then sent to the decoder to reconstruct the original image.

4.2. Generative Adversarial Network

As show in Figure 5(a), GAN [33] consist of two neural networks that are trained in an adversarial manner: a generator that to generate 'fake' data samples that are indistinguishable from the real data, and a discriminator that learns to distinguish between the generated and real data samples [34]. The generator generates new data samples by transforming a low-dimensional input noise vector into a high-dimensional output space that resembles the original data. The discriminator is trained to differentiate between the generated data and the real data. These two networks are optimized through a minimax game framework, wherein the generator aims to create data that can deceive the discriminator, while the discriminator strives to correctly classify the generated data as fake [14].

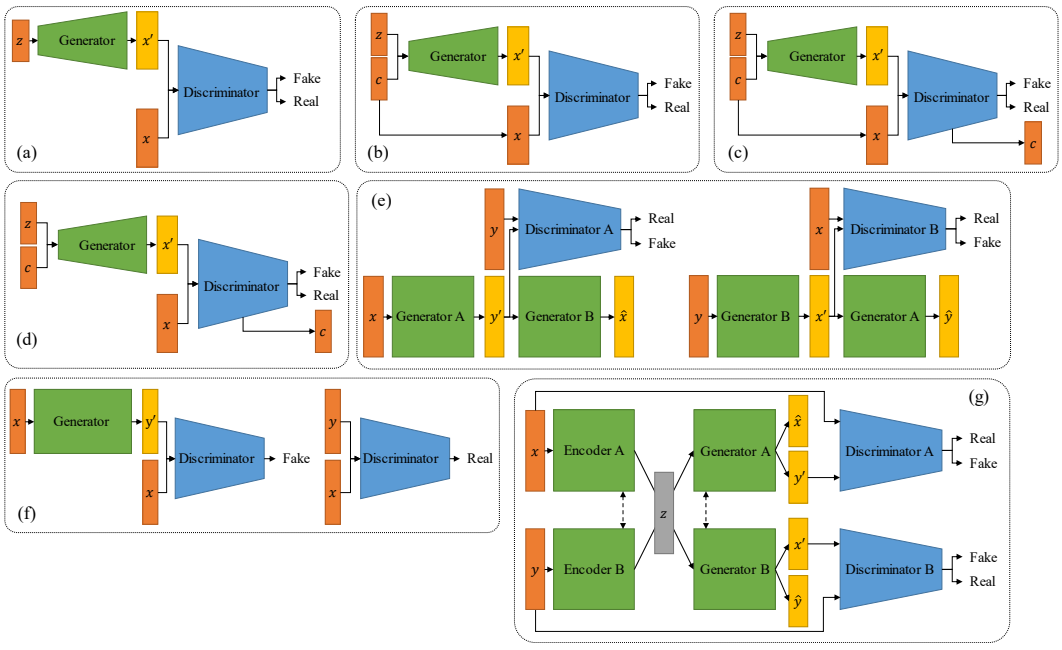

Figure 5. Architecture of GANs. (a) Vanilla GAN; (b) CGAN; (c) ACGAN; (d) InfoGAN; (e) CycleGAN; (f) Pix2Pix; (g) UNIT.

As show in Figure 5, variants of GANs have been proposed to address some of the challenges of traditional GANs. For example, conditional GANs (cGANs) add an additional input layer to the generator and discriminator networks, allowing the generator to generate data that satisfies specific conditions, such as class labels or image attributes. Similarly, deep convolutional GANs (DCGANs) use convolutional layers to learn hierarchical features from image data, improving the quality of the

 doi:10.20944/preprints202512.1407.v1

generated images. For image translation, Pix2Pix [35] and CycleGAN [36] are the two most commonly used models, and currently most medical image translation models are modified based on these two models [37–39]. GANs and their variants have shown remarkable success in various applications. However, they can be challenging to train and require careful tuning to avoid issues such as mode collapse and instability.

4.3. Diffusion Model

Diffusion models have been applied to various fields of image generation [34]. As show in Figure 6, the diffusion model is a type of probability generation model that gradually adds noise to the data to break the structure of the data, and then learns a corresponding reverse process to denoise, thereby learning the distribution of the original data. The forward diffusion process incrementally adds noise to the input data, progressively increasing the noise level until the data is entirely transformed into pure Gaussian noise. This process systematically disrupts the underlying structure of the data distribution. The reverse diffusion process, often referred to as denoising, is then employed to reconstruct the original data structure from the perturbed distribution. This step effectively reverses the degradation introduced by the forward diffusion process. As a result, a highly flexible and tractable generative model is achieved, capable of accurately modeling complex data distributions starting from random noise [34].

Recently, diffusion models and their variants have been applied to medical image analysis, include medical image creation [40,41], translation [42], reconstruction [43,44], denoising [45], registration [46], classification [47], and segmentation [48,49].

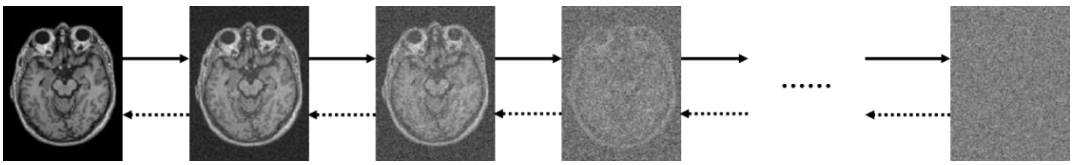

Figure 6. Architecture of diffusion model.

5. Creation

Due to the inherent structural complexity and large parameter scale of deep learning models, a significant amount of labeled data is typically required for their effective training. The acquisition of labeled medical image data heavily depends on the subjective expertise and professional judgment of radiologists [50]. Additionally, it is susceptible to issues related to image quality, leading to significant challenges such as data scarcity, insufficient annotations, and pronounced class imbalances. These limitations significantly hinder the broader adoption of deep learning models and represent a critical obstacle in the development of deep learning-based medical diagnostic systems [15].

Medical image data augmentation serves as a technique employed to augment the quantity and diversity of available medical images for training machine learning models [16]. Traditional data augmentation techniques include methods such as image quality enhancement, adjustments to brightness or contrast, and geometric transformations like rotation, scaling, and deformation [15]. The ascendancy of deep learning-based generative models in the synthesis of data has garnered substantial attention. Within the domain of medical image analysis, the utilization of deep learning-based generative models for the generation of medical image data assumes paramount significance. This approach can simulate a substantial volume of challenging-to-obtain medical image data, effectively mitigating the adverse impact of data scarcity on the domain of medical image analysis [22].

In this section, we summarize the application of generative models in medical image creation. We review the literature based on downstream tasks, namely classification tasks, segmentation tasks, and other tasks. As shown in Figure 7(a), it is used for creating medical image data for classification

 doi:10.20944/preprints202512.1407.v1

tasks. Specifically, various classes of medical images are created from random noise, and then the created data is used to train a classification model. Figure 7(b) is used for creating medical image data for segmentation tasks. Medical images are created from segmentation masks, and then the created data and masks are used to train a segmentation model. Figure 7(c) is used for creating medical image data for other downstream tasks, such as regression, object detection, and survival prediction.

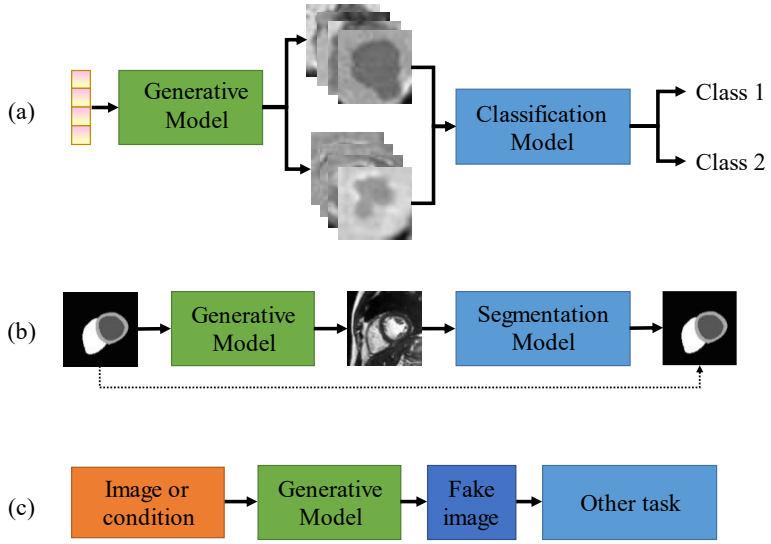

Figure 7. Creation for downstream tasks. (a) Creation for classification. (b) Creation for segmentation. (c) Creation for other tasks.

5.1. Metrics of Medical Image Creation

In order to verify the performance of the proposed medical image creation method, it is necessary to use metrics to evaluate the similarity between the synthesized image. Table 1 lists several commonly used image similarity evaluation metrics. $\mathbb{P}_r$ denotes the real image distribution, $\mathbb{P}_g$ denotes the generated image distribution. $p_{\mathcal{M}}(y|x)$ denotes the label distribution of x as predicted by $\mathcal{M}$, and $p_{\mathcal{M}}(y) = \int p_{\mathcal{M}}(y|x)\, d\mathbb{P}_g$. $p_{\mathcal{M}}(y^*) = \int p_{\mathcal{M}}(y|x)\, d\mathbb{P}_r$ is the marginal label distribution for the samples from the real data distribution.$\Gamma(\mathbb{P}_r, \mathbb{P}_g)$ denotes the set of all joint distributions (i.e., probabilistic couplings) whose marginals are respectively $\mathbb{P}_r$ and $\mathbb{P}_g$, and $d(x_r, x_g)$ denotes the base distance between the two samples.

Table 1. Quantitative evaluation metrics of medical image creation.

Symbol	Name	Formula
IS	Inception Score	$\mathrm{IS}(\mathbb{P}_g) = e^{\mathbb{E}_{x\sim\mathbb{P}_g}[KL(p_{\mathcal{M}}(y\|x)\|\|p_{\mathcal{M}}(y))]}$
MS	Mode Score	$\mathrm{MS}(\mathbb{P}_g) = e^{\mathbb{E}_{x\sim\mathbb{P}_g}[KL(p_{\mathcal{M}}(y\|x)\|\|p_{\mathcal{M}}(y))]-KL(p_{\mathcal{M}}(y)\|\|p_{\mathcal{M}}(y^*))}$
MMD	Kernel Maximum Mean Discrepancy	$\mathrm{MMD}(\mathbb{P}_r, \mathbb{P}_g) = \mathbb{E}_{\substack{x_r,x_r'\sim\mathbb{P}_r,\\ x_g,x_g'\sim\mathbb{P}_g}}[k(x_r, x_r') - 2k(x_r, x_g) + k(x_g, x_g')]$
WD	Wasserstein distance	$\mathrm{WD}(\mathbb{P}_r, \mathbb{P}_g) = \inf_{\gamma\in\Gamma(\mathbb{P}_r,\mathbb{P}_g)}\mathbb{E}_{(x_r,x_g)\sim\gamma}[d(x_r, x_g)]$
FID	Fréchet Inception Distance	$\mathrm{FID}(\mathbb{P}_r, \mathbb{P}_g) = \|\mu_r - \mu_g\| + \mathrm{Tr}(\mathrm{C}_r + \mathrm{C}_g - 2(\mathrm{C}_r\mathrm{C}_g)^{1/2})$

The Inception Score (IS) uses a pre-trained Inception-v3 model to compute the KL-divergence between the predicted class distributions of generated images and their overall diversity [51]. A higher IS indicates better image quality and diversity. The Mode Score (MS) adds a measure of similarity between the probability distributions of generated samples and real samples based on the IS. Kernel Maximum Mean Discrepancy (MMD) quantifies the difference between the probability distributions of generated samples and real samples using a fixed kernel function. Wasserstein

 doi:10.20944/preprints202512.1407.v1

Distance (WD) serves as a metric to evaluate the similarity between two distributions, where a smaller WD indicates greater similarity. Fréchet Inception Distance (FID) computes the Wasserstein-2 distance between the distributions of feature vectors derived from generated and real images, utilizing a pre-trained Inception-v3 model for feature extraction [51]. A lower FID indicates better image quality.

5.2. Classification

In recent years, there have been notable developments in medical image classification techniques, driven by advancements in deep learning algorithms [52]. However, several challenges and limitations remain. First, acquiring large-scale medical image datasets is often difficult due to privacy concerns, limited accessibility, and ethical constraints. Second, training medical image classification models necessitates the involvement of expert radiologists, pathologists, or clinicians to manually annotate the images with appropriate labels or categories. This annotation process is not only labor-intensive but also requires specialized expertise, creating significant barriers to effectively training deep learning models. Third, medical datasets frequently exhibit class imbalance, where certain disease categories are underrepresented compared to others, further complicating model training and evaluation [53]. Detecting rare diseases or conditions with limited training samples poses a challenge, as models tend to favor the majority classes during training.

In this section, we undertake a comprehensive review of the pertinent literature about medical image creation for classification. We compile essential information from the literature and present it in Table 2.

Table 2 provides a comprehensive overview of 27 literature sources, with most of them being based on GAN. Among these 27 sources, the highest number of publications is focused on chest, with 14 of them specifically targeting chest-related studies. The most common application is in the generation of X-ray and CT images. Additionally, most of the literature is based on 2D models, possibly due to limitations in GPU memory.

Pesteie et al. [30] introduced a variational generative model to learn the probability distribution of image data conditioned on latent variables and corresponding labels. The trained model is employed to generate new images for data augmentation. The efficacy of this approach is demonstrated through its application to ultrasound images (US) of the spine and brain MRI. This model resulted in a notable enhancement in the accuracy of the classification task.

Salehinejad et al. [54] proposed a DCGAN to create synthesized chest X-rays. They utilized both real and synthesized images to train a model for the detection of pathology across five classes of chest X-rays. A comparative analysis of DCNNs trained with a mixture of real and synthesized images revealed that the model outperformed its counterparts trained exclusively with real images.

Pan et al. [55] proposed an image synthesis framework based on diffusion model utilizing a Swin-transformer-based network. This model encompasses a forward Gaussian noise process and a reverse process employing the transformer-based diffusion model for denoising. COVID-19 classification models were trained using real images, synthetic images, and combinations of both.

Applying generative model-based data augmentation methods to medical image classification tasks offers several advantages. First, generative models can learn the underlying data distribution and produce synthetic samples that closely resemble real images. These generated samples can be used to augment the original dataset, enhancing the performance and robustness of classification models [56]. Second, medical image datasets often exhibit class imbalance, where certain disease categories are underrepresented. Synthesis algorithms can generate synthetic samples for these minority classes, helping to balance the class distribution and reduce bias toward majority classes during training. Third, synthesis algorithms can introduce intra-class variations by creating diverse samples with different appearances, shapes, or textures. This enables the model to learn more robust and discriminative features, improving its ability to generalize to unseen data. Furthermore, medical datasets are often limited due to privacy concerns, the rarity of certain conditions, or the high costs associated with data acquisition [57]. Synthesis algorithms allow researchers to artificially expand the

 doi:10.20944/preprints202512.1407.v1

dataset by generating additional samples, effectively increasing the amount of training data available for the classification task. In conclusion, by leveraging synthesis algorithms for data augmentation, medical image classification models can benefit from increased dataset size, improved class balance, intra-class diversity.

5.3. Segmentation

Developing a medical image segmentation model necessitates the expertise of radiologists or clinical professionals to manually annotate the images, thereby establishing ground truth data that serves as a reference for training and evaluating the segmentation model [58]. Manual annotation is a time-intensive, subjective process reliant on expert knowledge, rendering the task of constructing extensive and diverse datasets a formidable endeavor.

The generative models provide the images and masks required for training medical image segmentation models by converting masks into synthetic images. This approach significantly mitigates the demand for annotated data. In this section, we embark on an exhaustive review of the pertinent literature, which we present comprehensively in Table 3.

Table 3 offers a comprehensive overview of 26 literature sources, with the majority of them centering on GAN. Similar to the emphasis on data creation for classification tasks, a significant number of publications focus on chest and lung-related topics. The most prevalent applications involve the generation of X-ray, CT, and ultrasound images. As same as creation for classification, most of the literature is based on 2D models.

Guo et al. [59] introduced a confidence-guided synthesis of anatomic and molecular MR image networks (CG-SAMR) that enables the synthesis of data by leveraging lesion contour information into multi-modal MR images. Additionally, they extended the proposed architecture to support training with unpaired data. The synthesized data proves valuable for data augmentation, especially in the context of images containing pathological information related to gliomas.

Zhang et al. [60] presented an improved Dense GAN for data augmentation. They harnessed the power of Dense GAN to generate CT images, facilitating effective semi-supervised segmentation.

Amirrajab et al. [61] proposed a method for synthesizing cardiac MR images with plausible heart shapes and appearances to create labeled data. The approach dissects image synthesis into two tasks: label deformation and label-to-image translation. Label deformation is achieved through latent space interpolation within VAE model, while label-to-image translation is accomplished using a conditional GAN.

5.4. Other Tasks

In addition to classification and segmentation tasks, there are other tasks in the field of medical image analysis, such as regression, object detection, and survival prediction. There are currently many proposed data augmentation methods based on generative models for these tasks. We compile essential information from the literature and present it in Table 4. In addition, we also collected some literature without specified downstream tasks, and they are all listed in Table 4.

Han et al. [62] introduced a 3D Multi-Conditional GAN (MCGAN) to generate nodules on lung CT images to enhance sensitivity in object detection. The MCGAN incorporates two discriminators: the context discriminator and the nodule discriminator. The results demonstrate that 3D CNN-based detection achieves increased sensitivity for nodules of any size or attenuation at fixed False Positive rates, effectively addressing the scarcity of medical data by leveraging MCGAN-generated realistic nodules.

Kamli [63] proposed a Synthetic Medical Image Generator (SMIG) with the primary aim of generating synthetic MRI using GAN to provide anonymized data. Furthermore, to predict the growth of glioblastoma multiform tumors, the authors developed a tumor growth predictor. The authors emphasized the significance of employing synthetic data generated by SMIG. Despite the limited dataset size available from public dataset, the results demonstrate valuable accuracy in predicting tumor growth.

 doi:10.20944/preprints202512.1407.v1

Li et al. [64] introduced DeepAnat, a method to synthesize high-quality T1 images from diffusion MRI and to perform brain segmentation on synthesized T1 images and assist co-registration using synthesized T1 images. This study underscores the advantages and practical feasibility of creating medical images to support various diffusion MRI data analyses and their utility in neuroscientific applications.

Table 2. The studies on medical image creation for the classification task.

Paper	Model	Anatomy	Modality	Dimension
[65]	DCGAN, ACGAN	Liver	CT	2D
[66]	DCGAN, WGAN, BEGAN	Thyroid	OCT	2D
[67]	ACGAN	Limb	X-ray	2D
[30]	ICVAE	Spine, brain	Ultrasound, MRI	2D
[54]	DCGAN	Chest	X-ray	2D
[68]	-	Lung	CT	3D
[69]	PGGAN	Chest	X-ray	2D
[70]	MTT-GAN	Chest	X-ray	2D
[71]	CT-SGAN	Chest	CT	3D
[72]	COViT-GAN	Chest	CT	2D
[73]	Two stage GAN	Liver	Ultrasound	2D
[74]	TripleGAN	Breast	Ultrasound	2D
[75]	InfoGAN	Lung	CT	2D
[76]	GAN	Chest	X-ray	2D
[77]	LSN	Brain	CT	2D
[78]	StyleGAN2	Chest	X-ray	2D
[79]	DCGAN, cGAN	Prostate	MRI	2D
[80]	TMP-GAN	Breast, pancreatic	X-ray, CT	2D
[81]	CycleGAN	Chest	X-ray	2D
[82]	PLGAN	Ophthalmology, Brain, Lung	OCT, MRI, CT, X-ray	2D
[83]	CUT	Chest	X-ray	2D
[84]	HBGM	Coronary	X-ray	2D
[85]	DC-GAN	Chest	X-ray	2D
[86]	MI-GAN	Chest	CT	2D
[87]	StyleGAN2	Chest	X-ray	2D
[55]	DDPM	Chest, heart, pelvis, abdomen	MRI, CT, X-ray	2D
[88]	StynMedGAN	Chest, brain	MRI, CT, X-ray	2D

Table 3. The studies on medical image creation for the segmentation task.

Paper	Model	Anatomy	Modality	Dimension
[89]	Two stage GAN	Intravascular	Ultrasound	2D
[90]	SpeckleGAN	Intravascular	Ultrasound	2D
[91]	CycleGAN	Gastrocnemius medialis muscle	Ultrasound	2D
[92]	Private	-	-	2D
[93]	Pix2Pix	bone surface	Ultrasound	2D
[31]	VAE	-	Ultrasound	2D
[94]	Pix2Pix	Prostate	MRI	2D
[59]	CG-SAMR	Brain	MRI	3D
[95]	GAN, VAE	Thyroid	Ultrasound	2D
[96]	WFT-GAN	-	-	2D
[60]	Dense GAN	Lung	CT	2D

 doi:10.20944/preprints202512.1407.v1

[61]	VAE, GAN	Cardiac	MRI	3D
[97]	LEGAN	Retinal	Digital Retinal Images	2D
[98]	spGAN	Lung, hip joint, ovary	Ultrasound	2D
[99]	cGAN	cardiac	MRI	2D
[100]	SR-TTT	Liver	CT	2D
[101]	Pix2Pix, CycleGAN, SPADE	Brain	MRI	2D
[102]	SPADE	Rectal	MRI	3D
[103]	3D GAN	Lung	CT	3D
[104]	-	Lung	X-ray	2D
[105]	-	Brain	MRI	3D
[106]	DCGAN	Retinal, coronary, knee	X-ray, MRI	2D
[107]	Pix2Pix	Lung	CT	2D
[108]	-	Cheat	X-ray	2D
[109]	Pix2Pix	Lung	CT	2D
[110]	MinimalGAN	Retinal fundus	Nature	2D

Table 4. The studies on medical image creation for other tasks.

Paper	Model	Anatomy	Modality	Dimension	Task
[111]	DCGAN, WGAN	Brain	MRI	2D	None
[62]	MCGAN	Lung nodules	CT	3D	Object detection
[63]	SMIG	Brain glioblastoma	MRI	3D	Tumors growth prediction
[112]	InfoGAN	Fetal head	Ultrasound	2D	None
[113]	Private	Prostate	MRI	2D	Prostate cancer Localization
[114]	DCGAN-PSO	Lung	X-ray	2D	None
[115]	U-Net	Lung nodules	X-ray	2D	Object detection
[116]	3D-StyleGAN	Brain	MRI	3D	None
[117]	CGAN, DCGAN, f-GAN, WGAN, CycleGAN	Lung	X-ray, CT	2D	None
[118]	DCGAN	Brian	MRI	2D	None
[64]	DeepAnat	Brian	MRI	3D	Neuroscientific applications

6. Translation

Medical image modality translation refers to the process of converting images from one or more modalities into different modalities [119], such as transforming from CT to MRI or from T1 and T2 to FLAIR. Medical image modality translation proves invaluable when medical imaging data is scarce or when patients cannot undergo specific imaging modalities due to medical or technical constraints. Modality translation empowers medical professionals and researchers to access more comprehensive information about a patient's medical condition, enhancing the accuracy of diagnosis and treatment planning [18].

Conventional methods entail the utilization of models with predefined rules to effectuate the conversion of images from one modality to another. These models necessitate manual parameter adjustments to achieve optimal performance and are often tailored to specific applications, contingent upon the distinctive characteristics of the involved imaging modality [18]. Consequently, numerous intricate and application-specific techniques have been developed. However, these methods confront challenges when the two imaging modalities provide disparate information, rendering the establishment of an effective model a formidable undertaking.

In tandem with the advancement of deep learning, an increasing array of modality translation methods grounded in deep learning principles have emerged. Deep learning-based generative

 doi:10.20944/preprints202512.1407.v1

models, exemplified by GANs and diffusion models, have exhibited tremendous potential in the domain of medical image modality translation [20]. They excel by acquiring the capability to learn the mapping between different modalities and generating high-quality synthetic images.

In this section, we classify the collected modality translation literature according to the target modality. In Figure 8, the literature quantity is shown for translations between CT, MRI, CBCT, X-ray, PET, and ultrasound image. The number of studies of the six source modalities is in the order of MRI (63), CT (18), CBCT (15), PET (7), X-ray (3) and US (1). The number of studies of the six targeted modalities is in the order of CT (78), MRI (18), PET (6), X-ray (4), US (1). There are four kinds of translations worthy attention. The first is the translation from MRI to CT (59 studies), primarily focusing on dose calculation for MRI-guided radiation therapy. The second is the translation from CT to MRI (13 studies), primarily aiming for more accurate segmentation. The third is the translation from CBCT to CT with the main objective of 12, primarily serving the objectives of image denoising and dose calculation. The fourth is to translate PET to CT specifically for attenuation correction.

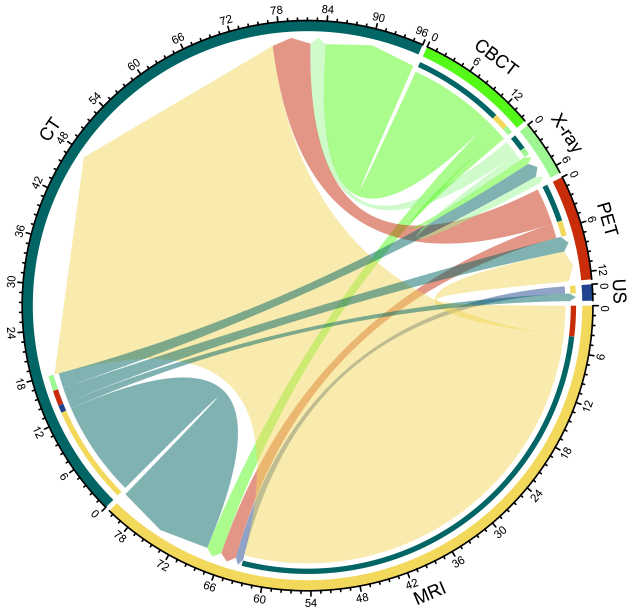

Figure 8. Chord diagram of medical image translation cross modalities of MRI, CT, CBCT, X-ray, PET, and US.

In addition, the translation between non-contrast images and contrast images has also been a research hotspot in recent years, and we will separately organize them in Section 6.7.

6.1. Metrics of Medical Image Translation

In order to verify the performance of the proposed modality translation method, it is necessary to use metrics to evaluate the similarity between the synthesized image and the real image. Table 5 lists several commonly used image similarity evaluation metrics.

Mean Absolute Error (MAE) provides a straightforward, easy-to-interpret measurement of error. It gives equal weight to all errors, regardless of their magnitude, making it less sensitive to outliers. Mean Squared Error (MSE) gives a more significant penalty to large errors compared to MAE, which can be desirable in some contexts. It is also widely used and mathematically convenient. Peak Signal-to-Noise Ratio (PSNR) is based on MSE and shares some of its limitations [120]. It does not always align with human perception, especially for complex images or artifacts like blockiness. Structural Similarity Index (SSIM) is designed to measure the similarity between two images in terms of luminance, contrast, and structure, which aligns better with human perception [121]. It is often

 doi:10.20944/preprints202512.1407.v1

considered more accurate than PSNR for evaluating image quality. In summary, MAE and MSE are simple and widely used metrics that are easy to compute but may not always align with human perception. PSNR is also widely used and easy to interpret but may not correlate well with perceptual quality. SSIM, on the other hand, is more aligned with human perception but can be more computationally expensive. Choosing the right metric depends on the specific requirements of the application and the aspects of image quality that are most important.

Table 5. Quantitative evaluation metrics of medical image translation.

Symbol	Name	Formula
MAE	Mean Absolute Error	$\frac{1}{m}\sum_{i=1}^{m}\lvert y_i - x_i\rvert$
MSE	Mean Square Error	$\frac{1}{m}\sum_{i=1}^{m}(y_i - x_i)^2$
RMSE	Root Mean Square Error	$\sqrt{MSE}$
PSNR	Peak Signal-to-Noise Ratio	$20 \cdot \log_{10}(\frac{\mathrm{MAX}}{RMSE})$
SSIM	Structural similarity index	$\frac{(2\mu_x\mu_y + \mathrm{C}_1)(2\sigma_{xy} + \mathrm{C}_2)}{(\mu_x^2 + \mu_y^2 + \mathrm{C}_1)(\sigma_x^2 + \sigma_y^2 + \mathrm{C}_2)}$

In the equations in Table 5, x_i and y_i are the pixel values of position i in the image x and y, respectively. MAX is the maximum possible pixel value. μ_x and μ_y are the mean value of image x and y, respectively. σ_x^2 and σ_y^2 are the variance of image x and y, respectively. σ_{xy} is covariance of image x and y. C_1 and C_2 are constants.

6.2. Generating MRI

6.2.1. Multi-Contrast MRI Synthesis

MRI stands as a non-invasive medical imaging technique utilizing a potent magnetic field and radio waves to generate intricate images of internal organs and tissues within the human body [38]. Various MRI modalities, including T1-weighted (T1w), T2-weighted (T2w), Diffusion-Weighted Imaging (DWI), Magnetic Resonance Angiography (MRA), and Fluid-Attenuated Inversion Recovery (FLAIR), offer distinctive characteristics and applications. In tumor analysis, T1-weighted scans excel at differentiating gray and white matter in brain images, while T2-weighted images enhance the contrast between fluid and cortical tissue. FLAIR (Fluid-Attenuated Inversion Recovery) sequences are particularly effective in suppressing cerebrospinal fluid signals, improving lesion visibility. T1 contrast-enhanced (T1ce) images are valuable for delineating tumor regions in brain scans. Magnetic Resonance Angiography (MRA) is primarily used to evaluate vascular anatomy and detect abnormalities that may predispose to hemorrhages. Proton density (PD) images are widely utilized in radiology for inferring water content, aiding in lesion classification and multispectral segmentation. The integration of these multimodal MRI scans provides complementary information, with each modality offering unique insights into the body's internal structures and functions. Together, they deliver a comprehensive assessment of the patient's condition [38].

In some cases, it may be difficult to collect complete modalities for medical image analysis due to factors such as the cost of long-term examinations and uncooperative patients, particularly children and the elderly [122]. In such situations, synthesizing missing or damaged modalities using successfully acquired modalities can improve the availability of diagnosis-related images and enhance analysis tasks such as classification and segmentation. In recent years, with the development of deep learning based generative models, there has been an increasing amount of work on the translation between MRI modalities. Table 6 lists essential information of these works.

 doi:10.20944/preprints202512.1407.v1

In Figure 9(a), based on the number of studies, the primary translations can be ranked as T1-to-T2 (17), T2-to-T1 (13), T1-to-FLAIR (10), T2-to-PD (7), T2-to-FLAIR (6), PD-to-T2 (6), FLAIR-to-T1 (4), FLAIR-to-T2 (4), T1-to-PD (2), PD-to-T1 (2), T2-to-DWI (2), and DWI-to-T2 (1). In Figure 9(b), according to the number of studies, the main translations can be ranked as (T1, FLAIR)-to-(T2, T1ce) (4), (T1, T1ce)-to-(T2, FLAIR) (4), (T1, T2)-to-(T1ce, FLAIR) (4), (T1ce, FLAIR)-to-(T1, T2) (4), (T2, FLAIR)-to-(T1, T1ce) (4), and (T2, T1ce)-to-(T1, FLAIR) (4). In Figure 9(c), the main translations are T1-to-(T2, T1ce, FLAIR) (4), T2-to-(T1, T1ce, FLAIR) (4), FLAIR-to-(T1, T2, T1ce) (4), and T1ce-to-(T1, T2, FLAIR) (4). In Figure 9(d), the primary translations are (T1, T1ce, FLAIR)-to-T2 (7), (T1, T2, FLAIR)-to-T1ce (7), (T1, T2, T1ce)-to-FLAIR (7), and (T2, T1ce, FLAIR)-to-T1 (7). The fundamental objective of MRI image translation across contrast mechanisms is to avoid the acquisition of actual scans and provide the unavailable MRI modality necessary for diagnosis and treatment.

In most cases, as the number of source modalities increases, the model's performance tends to improve. On the same dataset, the performance of multi-to-single translation is superior to single-to-single translation. This is because more modalities can provide complementary information to each other, leading to a more realistic target modality. However, when the number of source modalities remains the same and the number of target modalities increases, no fixed trend in performance has been observed.

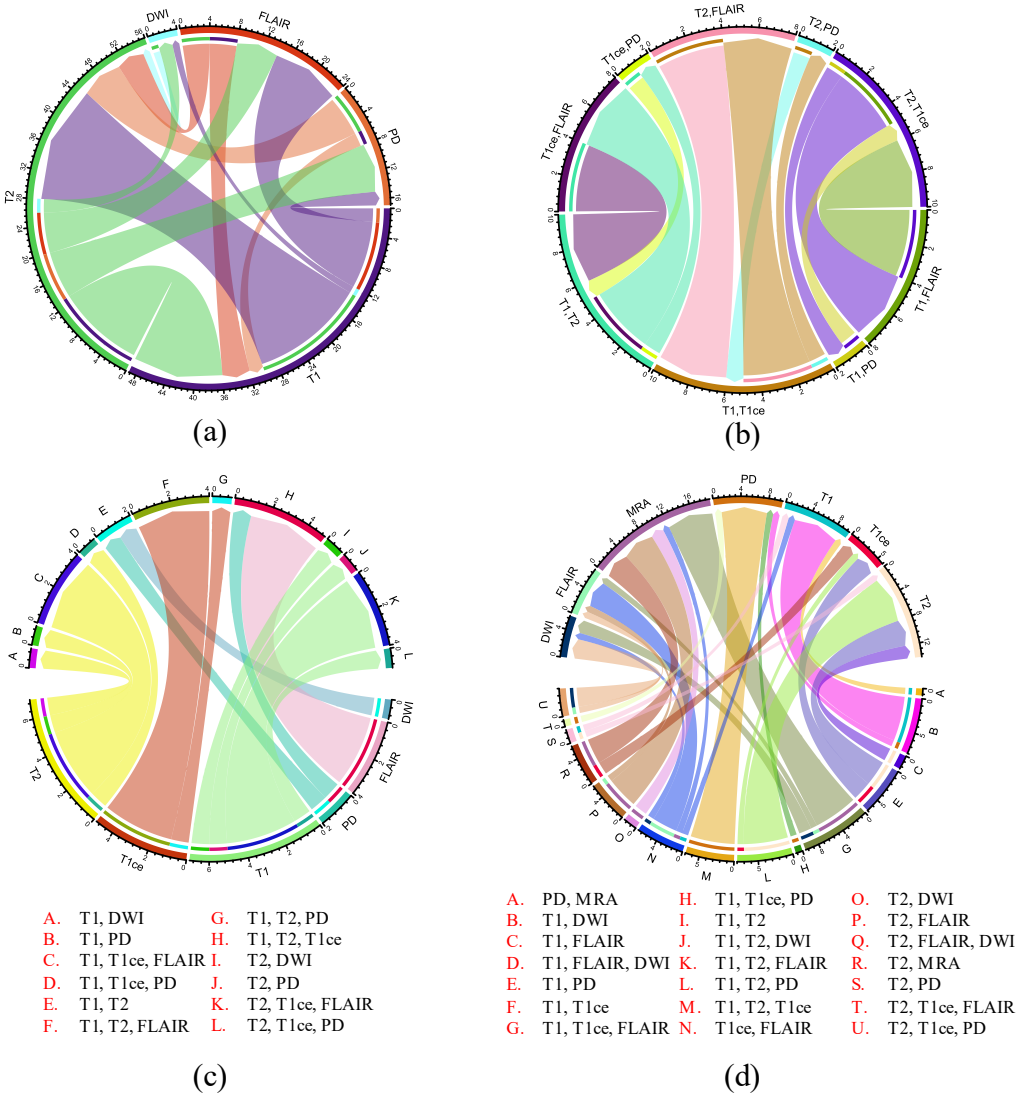

Figure 9. Chord diagram of MRI image translation across contrast mechanisms. (a) Single-to-single translation; (b) Multi-to-multi translation; (c) Single-to-multi translation; (d) Multi-to-single translation.

 doi:10.20944/preprints202512.1407.v1

As show in Table 6, there are several widely used datasets in cross-modality MRI translation, such as IXI, BraTS, and ISLES. The IXI dataset comprises nearly 600 MRIs obtained from normal and healthy subjects. The MRI acquisition protocol for each subject includes a comprehensive set of sequences: T1, T2, PD, MRA, and DWI. These data have been collected across three different hospitals. The Brain Tumor Segmentation (BraTS) dataset is a widely recognized and frequently used collection of medical images specifically designed for brain tumor research, particularly in the field of medical image analysis and machine learning. The dataset includes multimodal brain MRI scans, typically comprising T1, T1ce, T2, and FLAIR images. The Ischemic Stroke Lesion Segmentation (ISLES) challenge is dedicated to evaluating infarct segmentation in both acute and sub-acute stroke cases, leveraging multimodal MRI data. The inaugural ISLES challenge, held in 2015, was divided into two sub-challenges: Sub-acute Stroke Lesion Segmentation (SISS) and Stroke Perfusion Estimation (SPES). SISS aimed to segment subacute stroke lesions using conventional post-stroke MRI sequences, including T1, T2, FLAIR, and DWI. The ISLES 2018 challenge focused on predicting infarct core delineation in DWI using CT perfusion data. The primary objective of the ISLES 2022 challenge is to segment stroke lesions from DWI, ADC, and FLAIR sequences, with a dataset comprising 400 cases.

Currently, most methods are based on GANs, and most of these methods utilize 2D network architecture, possibly due to memory constraints. Furthermore, algorithms that require paired data for training are more prevalent than those that can use unpaired data because paired images can provide better supervision, leading to improved model performance.

Salman et al. [38] proposed pGAN and cGAN for multi-contrast MRI synthesis, leveraging conditional GANs. The proposed approach preserves intermediate-to-high frequency details through an adversarial loss, providing enhanced synthesis performance using pixel-wise and perceptual losses for registered multi-contrast images and a cycle-consistency loss for unregistered images.

Zhou et al. [123] introduced a Hybrid-fusion Network (Hi-Net) for multi-modal MRI synthesis, which learns a mapping from multi-modal source images to target images. In Hi-Net, a modality-specific network is employed to learn representations for each individual modality, and a fusion network is utilized to learn the common latent representation of multi-modal data. Subsequently, a multi-modal synthesis network is designed to densely combine the latent representation with hierarchical features from each modality, acting as a generator to synthesize the target images.

Muzaffer et al. [42] proposed SynDiff, employing adversarial diffusion model for multi-contrast MRI translation. To capture a direct correlate of the image distribution, SynDiff utilizes a conditional diffusion process that progressively maps noise and source images onto the target image. For efficient and accurate image sampling during inference, large diffusion steps are taken with adversarial projections in the reverse diffusion direction.

6.2.2. Generating MRI from Other Modalities

In this section, we summarize the papers on the translation from non-MRI modalities to MRI. The number of papers of CT-to-MRI is the highest. Table 7 lists essential information of these works.

Wang et al. [124] introduced a bidirectional learning model, denoted as dual contrast CycleGAN (DC-CycleGAN), designed to synthesize MRI from CT. Specifically, a dual contrast loss is incorporated into the discriminators to indirectly establish constraints between real source and synthetic images. This is achieved by leveraging samples from the source domain as negative samples, enforcing the synthetic images to diverge significantly from the source domain. Additionally, cross-entropy and the structural similarity index (SSIM) are integrated into the DC-CycleGAN to consider both the luminance and structure of samples during image synthesis.

Lei et al. [125] proposed a method generating MRIs with superior soft-tissue contrast from CBCT images to aid CBCT segmentation. The entire segmentation process comprises three major steps. Firstly, CycleGAN is utilized to estimate a synthetic MRI (sMRI) from CBCT images. Secondly, a deep attention network is trained based on sMRI and its corresponding manual contours. Finally,

 doi:10.20944/preprints202512.1407.v1

segmented contours for a query patient are obtained by feeding the patient's CBCT images into the trained sMRI estimation and segmentation model.

Bazangani et al. [126] proposed a separable convolution-based Elicit Generative Adversarial Network (E-GAN). The architecture can generate 3D T1 weighted MRI corresponding to FDG-PET

Table 6. The studies on the multi-contrast MRI translation.

Paper	Dataset	Dimension	Modality translation	Model	
				Name	Paired image
[127]	BraTS 2015	3D	T1→FLAIR	3D cGAN	Yes
[38]	MIDAS, IXI, BraTS	2D	T1↔T2	pGAN, cGAN	Yes, No
[128]	BraTS 2015, IXI	3D	T1→FLAIR; T1→T2	Ea-GANs	Yes
[129]	BraTS 2018	2D	T1, T2, T1ce, FLAIR (Three-to-One)	Auto-GAN	Yes
[122]	ISLES 2015, BraTS 2018	2D	T1, T2, DWI; T1, T1ce, T2, FLAIR (generating the missing contrast(s))	MM-GAN	Yes
[130]	BraTS 2018	2D	T1↔T2	-	Yes
[131]	Private	2D	T1↔T2	CACGAN	No
[132]	BraTS 2018	2D	T2→(FLAIR, T1, T1ce)	TC-MGAN	Yes
[133]	BraTS 2015, SISS 2015	3D	T1→FLAIR; T1→T2	SA-GAN	Yes
[123]	BraTS 2018	2D	T1↔T2; T1↔FLAIR; T2↔FLAIR; T1, T2, FLAIR (Two-to-One)	Hi-Net	Yes
[134]	BraTS 2017, TCGA	2D	(T1ce, FLAIR)→T2	-	Yes
[135]	BraTS 2018	2D	T1, T2, T1ce, FLAIR (generating the missing contrast(s))	-	Yes
[136]	BraTS 2015	2D	T1→FLAIR; T1→T2	EP-IMF-GAN	Yes
[137]	HCP 500	2D	B0→DWI; B0, T2→DWI; B0, T1, T2→DWI	-	Yes
[138]	Private, IXI	2.5D	T1→T2	-	Yes
[139]	IXI	2D	T2↔PD	DiCyc	No
[140]	BraTS 2015	2D	T1↔T2	-	No
[141]	IXI, BraTS 2019	2D	Unified model	Hyper-GAN	Yes
[142]	IXI, ISLES	2D	T1↔T2; T1↔PD; T2↔PD; T1↔FLAIR; T2↔FLAIR; T1, T2, PD (Two-to-One); T1, T2, FLAIR (Two-to-One)	mustGAN	Yes
[143]	BraTS 2015	2D	T1, T1ce→FLAIR; T1, T2→FLAIR; T1, T1ce→T2	LR-cGAN	Yes
[144]	BraTS 2018	3D	T1, T2, T1ce, FLAIR (generating the missing contrast(s))	-	Yes
[145]	ADNI	2D	T1→CBV	DeepContrast	Yes
[146]	Private	2D	PD↔T2	-	No
[147]	IXI, BraTS	2D	T1, T2, PD (Two-to-One); T1, T2, FLAIR (Two-to-One) PD↔T2; FLAIR↔T2	ResViT	Yes
[97]	IXI	2D	T2→PD	TR-GAN	Yes
[148]	BraTS2019	3D	T1, T2, T1ce, FLAIR (generating the missing contrast(s))	CoCa-GAN	Yes
[149]	-	2D	T2↔DWI	CICVAE	No
[150]	BraTS2019	2D	T1→T2	NEDNet	Yes
[151]	BraTS, Brain, SPLP	2D	T1↔T2	Bi-MGAN	No
[152]	IXI, vivo brain dataset	2D	T1, T2, PD (Two-to-One);	ProvoGAN	Yes

 doi:10.20944/preprints202512.1407.v1

			T1, T2, T1ce, FLAIR (Three-to-One)		
[153]	BraTS 2015, IXI	2D	T1↔T2; T1→FLAIR; T2→FLAIR; T2↔PD	D2FE-GAN	Yes
[154]	dHCP, BCP	3D	T1↔T2	PTNet3D	Yes
[155]	BraTS 2018	2D	T1↔FLAIR; T1↔T2	DualMMP-GAN	No
[156]	BraTS 2020, ISLES 2015, CBMFM	2D	T1, T2, FLAIR, T1ce (Three-to-One); T1, T2, FLAIR, DWI (Three-to-One)	AE-GAN	Yes
[157]	Private	2D	T1→DWI; T2→DWI; T1, T2→DWI; T1→FLAIR; T2→FLAIR; T1, T2→FLAIR	GAN	Yes
[158]	IXI, BraTS 2021	2D	T1, T2, PD; T1, T1ce, T2, PD (generating the missing contrast(s))	MMT	Yes
[42]	BraTS, IXI	2D	T1↔T2; T1↔PD; T2↔PD; T1↔FLAIR; T2↔FLAIR	SynDiff	No
[159]	BraTS 2018, IXI	2D	PD, MRA, T2 (Two-to-One)	LSGAN	No
[160]	BraTS 2018, IXI	2D	PD, MRA, T2 (Two-to-One)	-	Yes
[161]	Private	2D	T1, T2, ADC, T1ce, FLAIR→CBV	-	Yes
[162]	MRM NeAt Dataset; Private	2D	T1↔T2	MouseGAN	No

Table 7. The studies on the image translation to MRI from other modalities.

Paper	Origin modality	Anatomy	Dataset	Dimension	Model	
					Name	Paired image
[163]	CT	Lung	NSCLC	2D	CycleGAN	No
[164]	CT	Brain	Private	2D	-	Yes
[165]	CT	Pelvis	Private	3D	CycleGAN	No
[166]	CT	Abdomen	Private	2D	Pix2Pix	Yes
[167]	CT	Brain	ADNI	3D	-	Yes
[168]	CT	Brain, Abdomen	Private	2D	BPGAN	Yes
[169]	CT	Liver	CHAOS	2D	TarGAN	Yes
[170]	CT	Pelvis	Private	3D	CycleGAN	No
[171]	CT	Head and neck	Private	2D	-	Yes
[96]	CT	Abdomen	CHAOS	2D	WFT-GAN	No
[146]	CT	Brain	Private	2D	-	No
[172]	CT	Prostate	Private	2D	PxCGAN	Yes
[124]	CT	Brain	From [173]	2D	DC-CycleGAN	No
[125]	CBCT	Prostate	Private	3D	CycleGAN	Yes
[174]	CBCT	Brain	Private	3D	TGAN	Yes
[175]	PET	Brain	Private	2D	-	Yes
[126]	PET	Brain	ADNI	3D	E-GAN	Yes
[176]	Ultrasound	Brain	INTERGROWTH-21st, CRL	2D	-	No

6.3. Generating CT

CT is a potent medical imaging technique that employs X-ray technology and computer processing to generate cross-sectional images of the human body. CT delivers highly detailed cross-sectional views of internal structures, allowing for precise examination and analysis of anatomical features, organs, and bones [177]. CT scanning plays a pivotal role in diagnosing a wide array of medical conditions, including traumatic injuries like fractures and internal hemorrhaging, as well as

 doi:10.20944/preprints202512.1407.v1

the detection and assessment of tumors, vascular disorders like aneurysms and blockages, lung diseases such as pneumonia and cancer, and neurological disorders like strokes, brain tumors, and related conditions [178,179].

However, it's imperative to consider potential risks associated with CT scans due to their use of ionizing radiation, particularly when repeated imaging is necessary [180]. Furthermore, CT serves as the primary imaging modality for radiation therapy, as it provides essential electron density data for dose calculations. While MRI excels in visualizing soft tissues and tumors, it lacks the tissue attenuation information required for accurate dose calculations in radiation therapy. The utilization of generative models to translate MRI into CT images is pivotal in enabling MRI-only radiotherapy, which can yield cost savings, reduce patient radiation exposure, and eliminate registration errors associated with using two distinct imaging modalities [181].

Cone Beam Computed Tomography (CBCT) represents an advanced medical imaging technique widely applied in fields such as dentistry and maxillofacial radiology [182]. CBCT employs a cone-shaped X-ray beam and a specialized detector to produce high-resolution, three-dimensional images of specific regions of interest within the human body, primarily focusing on the craniofacial area. Notably, CBCT offers the advantage of lower radiation doses, enhancing patient safety, while still delivering exceptional image clarity for detailed visualization of anatomical structures like teeth, bones, and soft tissues. However, CBCT does have inherent limitations, including lower contrast for soft tissues and reduced spatial resolution compared to conventional CT. Additionally, CBCT is more susceptible to metal artifacts, potentially compromising image quality when scanning patients with dental restorations or implants. Therefore, the development of generative models to translate CBCT images into CT is of considerable significance [183].

In this section, we provide a comprehensive summary of research papers related to the translation from various imaging modalities, including CBCT, MRI, PET, and X-Ray, into CT. Table 8 lists essential information of these works.

Zhang et al. [183] decomposed CBCT-to-CT synthesis into artifact reduction and intensity correction. They proposed a Multimodal Unsupervised Representation Disentanglement (MURD) learning framework that disentangles content, style, and artifact representations from CBCT and CT images in the latent space. MURD can synthesize different forms of images by recombining disentangled representations. Additionally, they introduced a multipath consistency loss to enhance structural consistency in synthesis and a multidomain generator to improve synthesis performance.

Dong et al. [184] proposed a 3D CycleGAN framework to synthesize CT images from non-attenuation corrected PET (NAC PET). The method learns a transformation that minimizes the difference between sCT, generated from NAC PET, and true CT. It also learns an inverse transformation such that the cycle NAC PET image generated from the sCT is close to the true NAC PET image.

Zhou et al. [185] proposed a multimodality MRI synchronous construction based deep learning framework from a single T1-weight image for MRI-guided radiation therapy (MRIgRT) synthetic CT (sCT) image generation. The network is primarily based on GAN with sequential subtasks of intermediate synthetic MRI generation and joint sCT image generation from the single T1 MRI. It comprises a multitask generator and a multibranch discriminator, where the generator consists of a shared encoder and a split multibranch decoder.

Table 8. The studies on the image translation to CT from other modalities.

Paper	Origin modality	Anatomy	Dataset	Dimension	Model	
					Name	Paired image
[186]	CBCT	Nasopharyngeal carcinoma	Private	2D	U-Net	Yes
[187]	CBCT	Head and neck	Private	2D	CycleGAN	No
[188]	CBCT	masseter	Private	2D	CycleGAN-based	No

 doi:10.20944/preprints202512.1407.v1

[177]	CBCT, MRI	Head and neck	Private	2D	U-Net	Yes
[189]	CBCT	Head and neck	Private	2D	U-Net	Yes
[190]	CBCT	Head and neck	Private	2D	USsCTU-net	No
[191]	CBCT	Head and neck, pelvic	Private	2D	Cycle-RCDC-GAN	Yes
[174]	CBCT, MRI	Brain	Private	3D	TGAN	Yes
[192]	CBCT	Head and neck, pelvic	Private	2D	DCC-GAN	No
[193]	CBCT	Brain	Private	2D	CGAN	Yes
[194]	CBCT	Abdomen	Private	2D	CycleGAN	No
[183]	CBCT	Lung	Private	2D	MURD	No
[184]	NAC-PET	Whole body	Private	3D	CycleGAN	No
[195]	NAC-PET	Whole body	Private	2D	Wasserstein GAN	Yes
[196]	PET	Whole body	Private	2D	U-Net	Yes
[197]	PET	Animal	Private	2D	-	Yes
[146]	PET, MRI	Brain, Whole body	Private	2D	-	No
[198]	X-Ray	Lung	LIDC-IDRI	2D-3D	X2CT-GAN	Yes
[199]	X-Ray	Lung	PadChest	2D-3D	X2CT-GAN	Yes
[200]	MRI	Brain	Private	2D	U-Net	Yes
[201]	MRI	Pelvis	Private	2D	Pix2Pix	Yes
[202]	MRI	Brain, Pelvis	ADNI, Private	3D	-	Yes
[203]	MRI	Brain, Prostate	Private	3D	DECNN	Yes
[204]	MRI	Whole body	Private	2D	CycleGAN	No
[205]	MRI	Prostate	Private	2D	U-Net, GAN	Yes
[206]	MRI	Pelvis	Private	3D	Dense-Cycle-GAN	No
[207]	MRI	Liver	Private	3D	CycleGAN	No
[208]	MRI	Brain	[209]	3D	hGAN	No
[210]	MRI	Pelvis	Private	2D	Pix2PixHD	Yes
[129]	MRI	Brain	ADNI	2D	Auto-GAN	Yes
[167]	MRI	Brain	ADNI	3D	-	Yes
[211]	MRI	Brain	Private	2D	Attention-GAN	Yes
[212]	MRI	Pelvis	Private	2D	-	Yes
[213]	MRI	Liver	Private	2D	U-Net	Yes
[214]	MRI	Brain	Private	2D	U-Net	Yes
[215]	MRI	Lumbar spine	SpineWeb	3D	CycleGAN	No
[168]	MRI	Brain, Abdomen	Private	2D	BPGAN	Yes
[181]	MRI	Brain, Abdomen	Private, CHAOS	2D	SC-CycleGAN	No
[216]	MRI	Brain	Han et al. and JUH dataset	2D	uagGAN	Yes
[217]	MRI	Lumbar Spine	Private	2D	CycleGAN	No
[169]	MRI	Liver	CHAOS	2D	TarGAN	Yes
[218]	MRI	Pseudo	Private	2D	U-Net, GAN	Yes
[219]	MRI	Abdomen	Private	2D	SA-GAN	Yes
[220]	MRI	Pelvis, thorax, abdomen	Private	2.5D	CycleGAN	No
[221]	MRI	Head and neck	Private	3D	Label-GAN	Yes
[222]	MRI	Head and neck	Private	2D	Multi-Cycle GAN	No
[223]	MRI	Abdomen	Private	2D	-	Yes
[171]	MRI	Head and neck	Private	2D	-	Yes
[139]	MRI	Brain	IXI, MA^{3}RS	2D	DiCyc	Yes
[224]	MRI	Brain	Private	2D	-	No

 doi:10.20944/preprints202512.1407.v1

[96]	MRI	Abdomen	CHAOS	2D	WFT-GAN	No
[225]	MRI	Brian	Private	3D	-	Yes
[226]	MRI	Head and neck	Private	2D	-	Yes
[147]	MRI	Pelvis	Private	2D	ResViT	Yes
[227]	MRI	Brain	RIRE	2D	GCG U-Net	Yes
[228]	MRI	Head	RIRE	2D	U-Net$_{E\text{-}SGA}$, cWGAN$_{E\text{-}SGA}$	Yes
[229]	MRI	Head	Private	3D	ResUNet	Yes
[230]	MRI	Abdomen	Private	2D	U-Net, cGAN	Yes
[231]	MRI	Brain	Private	2D	CycleGAN	Yes
[232]	MRI	Brain	Private	3D	cGAN	Yes
[233]	MRI	Pelvis	Gold Atlas	2D	Diffusion	Yes
[234]	MRI	Brain	GKRS	2D	Pix2Pix	Yes
[235]	MRI	Brain	Atlas project	2D	Pix2Pix	Yes
[236]	MRI	Pelvis	VMAT	3D	MD-CycleGAN	No
[156]	MRI	Brain	CBMFM	2D	AE-GAN	Yes
[237]	MRI	Brain	Private	2D	CycleGAN	No
[238]	MRI	Brain	Private	2D	AMSF-Net	Yes
[239]	MRI	Abdomen	CHAOS	2D	SSA-Net	No
[42]	MRI	Pelvis	Private	2D	SynDiff	No
[240]	MRI	Abdomen	Private	2D	Pix2Pix	Yes
[37]	MRI	Brain	ABCs	2.5D	DU-CycleGAN	No
[241]	MRI	Brain	From [173]	2D	DC-cycleGAN	No
[242]	MRI	Brain	MedPix, Private	2D	MSE-Fusion	Yes
[243]	MRI	Pelvis	From [244]	2D	RTCGAN	Yes
[245]	MRI	Abdomen	Private	3D	QACL	Yes
[185]	MRI	Head and neck	Private	2D	CMSG-Net	Yes

6.4. Generating X-Ray Image

In this section, we provide a comprehensive summary of research papers related to the translation from various imaging modalities into X-ray. A summarized overview of these works is presented in Table 9, highlighting essential information for reference.

Yuen et al.[249] introduced a CT-based Chest X-ray (CXR) synthesis framework, named ct2cxr, for data augmentation in pneumonia classification. Leveraging GANs and a customized loss function tailored for model training, the approach aims to preserve target pathology and maintain high image fidelity. The results indicate that CXR images generated through style mixing enhance the performance of general pneumonia classification models. Evaluation on a Covid-19 dataset demonstrates similar improvements over baseline models.

Huang et al. [247] proposed a sigmoid-based intensity transform, utilizing the nonlinear optical properties of X-ray films, to enhance image contrast in synthetic cephalograms generated from 3D volumes. Super-resolution deep learning techniques are explored to improve image resolution. For low-dose purposes, Pix2pix is introduced for 2D cephalogram synthesis directly from two cone-beam projections. An efficient automatic landmark detection method for synthetic cephalograms is proposed, combining LeNet5 and ResNet50.

Shen et al. [250] proposed a strategy for obtaining X-ray projection images at novel view angles without the need for actual projection measurements. Specifically, a Deep Learning-based Geometry-Integrated Projection Synthesis (DL-GIPS) framework is proposed for generating novel-view X-ray projections. The deep learning model extracts geometry and texture features from a source-view projection, then performs geometry transformation on the extracted features to accommodate the change in view angle. In the final stage, the X-ray projection in the target view is synthesized from the transformed geometry and shared texture features via an image generator.

 doi:10.20944/preprints202512.1407.v1

Table 9. The studies on medial image translation to X-Ray from other modalities.

Paper	Origin modality	Anatomy	Dataset	Dimension	Model	
					Name	Paired image
[246]	DRR	Chest	JSRT, NIH	2D	TD-GAN	No
[247]	CBCT	Head	CQ500	2D	Pix2Pix	Yes
[248]	CT	Chest	LIDC-IDRI, TBX11K	2D	XraySyn	No
[249]	CT	Chest	CheXpert	2D	CT2CXR	No
[250]	X-ray	Chest	LIDC-IDRI	2D	DL-GIPS	Yes

Table 10. The studies on the image translation to PET from other modalities.

Paper	Origin modality	Anatomy	Dataset	Dimension	Model	
					Name	Paired image
[251]	MRI	Brain	ADNI	3D	-	Yes
[252]	MRI	Brain	ADNI	2D	CL-GAN	Yes
[253]	MRI	Brain	ADNI	3D	BMGAN	Yes
[254]	MRI	Brain	ADNI	3D	BPGAN	Yes
[255]	CT	Liver	Private	2D	FCN-GAN	Yes
[146]	CT	Whole body	Private	2D	-	No

Table 11. The studies on the translation between in NC and CE images.

Paper	Modality	Translation	Anatomy	Dataset	Dimension	Model	
						Name	Paired image
[256]	MRI	NC to CE	Brain	IXI	2D	Steerable GAN	Yes
[257]	MRI	NC to CE	Cardiac	CycleGAN	2D	MS-CMRSeg	No
[258]	MRI	NC to CE	Liver	Private	2D	Tripartite-GAN	Yes
[259]	MRI	NC to CE	Brain	Private	3D	V-net	Yes
[260]	MRI	NC to CE	Ankylosing spondylitis	Private	2D	AMCGAN	Yes
[261]	MRI	NC to CE	Liver	Private	2D	Pix-GRL	Yes
[262]	CT	NC to CE	Aorta	Private	2D	Cascade GAN	Yes
[263]	CT	NC to CE	Aorta	Private	2.5D	aGAN	Yes
[264]	MRI	NC to CE	Brain	Private	3D	BICEPS	Yes
[265]	MRI	NC to CE	Brain	Private	3D	-	Yes
[266]	CT	NC to CE	Liver	Ircadb, Sliver07, LiTS	2D	-	Yes
[267]	CT	NC to CE	Cardiac	Private	2D	Pix2Pix	Yes
[268]	MRI	NC to CE	Breast	Private	2D	TSGAN	Yes
[39]	CT	Mutual synthesis	Lung	Private	3D	Pix2Pix	Yes
[269]	CT	Mutual synthesis	Lung	Coltea-Lung-CT-100W	2D	CyTran	No
[270]	CT	NC to CE	Kidney	Private	2D	CycleGAN	No
[271]	CT	NC to CE	Lung	LIDC-IDRI, EXACT09, CARVE14, PARSE	3D	CGAN	No
[272]	CT	NC to CE	Abdomen	CHAOS, Private	3D	UMTL	Yes

 doi:10.20944/preprints202512.1407.v1

6.5. Generating PET Image

Positron Emission Tomography (PET) is a powerful medical imaging technique. It is based on the principle of detecting and visualizing the distribution of positron-emitting radionuclides within the body [253]. PET imaging has a wide range of clinical applications. PET is used to detect and stage various types of cancers by highlighting areas with increased metabolic activity. PET is valuable in studying brain function and diagnosing conditions such as Alzheimer's disease, Parkinson's disease, and epilepsy. PET can assess blood flow and myocardial viability, helping in the evaluation of heart conditions, including coronary artery disease and myocardial infarction. PET is used to identify sites of infection or inflammation in the body, which can aid in the diagnosis and monitoring of infectious diseases and inflammatory disorders. PET allowing scientists to study various physiological processes, develop new drugs, and better understand diseases at the molecular level. PET provides functional and metabolic information, complementing the structural information obtained from techniques like CT and MRI [273]. It can detect diseases at an early stage when structural changes may not yet be apparent. PET has high sensitivity and specificity, making it a valuable tool for accurate disease detection and treatment monitoring [255].

Of course, PET also has some limitations. PET involves exposure to ionizing radiation due to the use of radiopharmaceuticals. It requires specialized equipment and trained personnel. PET scans may be expensive compared to some other imaging modalities. So, there is currently some work dedicated to converting other commonly used medical image modalities, such as MRI and CT, into PET. In this section, we provide a comprehensive summary of research papers related to the translation from CT or MRI into PET image. A summarized overview of these works is presented in Table 10, highlighting essential information for reference.

Hu et al. [253] introduced a 3D end-to-end synthesis network named Bidirectional Mapping GAN (BMGAN) for brain MR-to-PET synthesis, effectively utilizing image contexts and latent vectors. The proposed bidirectional mapping mechanism is designed to embed the semantic information of PET images into the high-dimensional latent space. Furthermore, the architecture includes a 3D Dense-UNet generator and hybrid loss functions to enhance the visual quality of cross-modality synthetic images.

Ben-Cohen et al. [255] combined a fully convolutional network (FCN) with a conditional GAN to simulate PET data from input CT data. From a clinical perspective, such solutions may facilitate lesion detection and drug treatment evaluation in a CT-only environment, potentially reducing the need for more expensive and radioactive PET/CT scans.

6.6. Generating Ultrasound Image

Ultrasound imaging is a non-invasive medical imaging technique that uses high-frequency sound waves to create real-time, dynamic images of the internal structures of the human body [274]. These images, known as ultrasound scans or ultrasound images, are valuable in medical diagnosis, monitoring pregnancies, and guiding various medical procedures.

Ultrasound imaging does not involve radiation or invasive procedures. It provides dynamic, real-time images, making it suitable for observing movement and function. Ultrasound is safe for pregnant women, infants, and individuals with contraindications to other imaging methods. Ultrasound machines come in various sizes, including handheld devices, making them highly portable for use in different clinical settings.

Grimwood et al. [275] proposed the use of CycleGAN to create synthetic Endoscopic ultrasound (EUS) images from CT data, that can be used as a data augmentation strategy when EUS data is scarce.

6.7. Non-Contrast and Contrast-Enhanced Image

Non-contrast enhanced medical imaging entails the acquisition of images without the administration of contrast agents. This imaging modality relies on the inherent contrast of natural

 doi:10.20944/preprints202512.1407.v1

tissues to visualize anatomical structures and identify potential abnormalities. Non-contrast imaging is commonly employed for routine screenings, initial assessments, and follow-up examinations. It is considered a safer option for patients with contraindications or allergies to contrast agents. Nonetheless, there are scenarios where non-contrast imaging may be limited, and the use of contrast-enhanced imaging could offer additional diagnostic insights.

Contrast-enhanced medical imaging involves the introduction of contrast agents, typically through intravenous administration, to enhance the visualization of specific anatomical structures or physiological processes [276]. These contrast agents contain substances that augment the visibility of blood vessels, organs, tumors, or regions with altered perfusion. Contrast-enhanced imaging proves particularly valuable in situations where non-contrast imaging may not provide adequate diagnostic information. For instance, in contrast-enhanced CT scans, iodine-based contrast agents are intravenously injected to accentuate blood vessels, tumors, and regions with abnormal blood flow, thereby improving the detection and characterization of lesions, vascular anomalies, and tumors. In contrast-enhanced MRI, gadolinium-based contrast agents are commonly utilized to enhance the visualization of blood vessels, brain tumors, and areas with compromised blood-brain barrier integrity, making it indispensable in neuroimaging and the diagnosis of conditions such as multiple sclerosis [277].

Contrast-enhanced imaging plays a pivotal role in diagnosing and characterizing various medical conditions, including tumors, vascular irregularities, inflammation, and ischemia. It furnishes critical insights into the dynamic behavior of tissues, enhancing the specificity and sensitivity of imaging investigations. However, certain patients may not be eligible for contrast agent injections due to various factors. To address this challenge, generative models can be employed to translate non-contrast enhanced images into contrast-enhanced images [278].

In this section, we provide an overview of research papers focused on the translation between non-contrast enhanced images and contrast-enhanced images. Table 11 presents essential details from these studies, offering a valuable reference for further exploration of this topic.

Zhao et al. [258] introduced a Tripartite Generative Adversarial Network (Tripartite-GAN) for synthesizing contrast-enhanced MRI (CEMRI) to detect tumors without the need for contrast agent injection. The Tripartite-GAN comprises three interconnected networks—an attention-aware generator, a convolutional neural network-based discriminator, and a region-based convolutional neural network-based detector. This integrated framework facilitates the synthesis of CEMRI and tumor detection, with the generator aiding accurate tumor detection by synthesizing tumor-specific CEMRI and the detector enhancing the generator for precise CEMRI synthesis through back-propagation.

Chen et al. [265] proposed a deep learning-based approach for contrast-enhanced T1 synthesis in brain tumor patients. A 3D high-resolution FCN designed to maintain high-resolution information and aggregate multi-scale information in parallel is employed to map pre-contrast MRI sequences (T1, T2, and ADC) to CEMRI sequences. To address data imbalance between normal tissues and tumor regions, a local loss is introduced to enhance the contribution of tumor regions, resulting in improved tumor enhancement.

Ristea et al. [269] presented a novel approach for translating NCCT scans to CECT scans and vice versa. The approach, named CyTran (cycle-consistent generative adversarial convolutional transformers), is trainable on unpaired images due to the integration of a multi-level cycle consistency loss. In addition to the standard cycle-consistency loss at the image level, additional cycle-consistency losses between intermediate feature representations are proposed, enforcing cycle-consistency at multiple representation levels, and leading to superior results. To handle high-resolution images, a hybrid architecture based on convolutional and multi-head attention layers is designed.

7. Discussion

This review provides a comprehensive summary of prior research on the utilization of generative models in the domain of medical image analysis. Through a synthesis of relevant

 doi:10.20944/preprints202512.1407.v1

literature, we categorize the applications of generative models in medical image analysis into two main segments: creation and translation. Building upon the diverse application scenarios of generative models in medical image analysis, this paper organizes previous studies into categories and offers practical implementation guidelines gleaned from the lessons learned in these works.

In Section 4, we conduct a thorough review of three widely employed generative models: VAEs, GANs, and diffusion models. We outline algorithms within these generative models that have found extensive applications in the domain of medical image analysis and provide analyses thereof.

In Section 5, we present an extensive review of creation methods. Depending on the downstream tasks, we classify creation's downstream applications into three distinct categories: classification, segmentation, and others. Among these, 27 studies focus on classification tasks, 26 studies on segmentation, and 11 studies on various other tasks. Our literature review consistently indicates that across various downstream tasks, data augmentation methods grounded in generative models consistently result in enhanced model performance, particularly when dealing with limited annotation resources.

Section 6 classifies translation methods based on the target modality. For the MRI modality, we identify 61 studies, with 42 studies primarily centered on inter-modal translation within MRI, particularly concentrated on brain images, while 19 studies encompass modalities such as CT, PET to MRI translation. Additionally, there are 77 studies for CT, 5 for X-ray, 6 for PET, and 1 for US, respectively. Furthermore, we conduct a separate analysis of 19 studies involving non-contrast enhanced and contrast-enhanced image translations.

Our comprehensive literature review underscores the notable advancements in GANs over recent years, with the majority of translation tasks predominantly relying on GAN-based methodologies. Furthermore, the introduction of DDPM has witnessed an increasing number of diffusion models being employed for translating medical images across different modalities. The remarkable image synthesis capabilities of diffusion models have significantly elevated the quality of synthesized images, albeit the inherent challenge of slow inference speed remains a critical concern [34].

Given the promising and rapidly evolving nature of medical image synthesis research, alongside the ongoing exploration of optimal image synthesis algorithms, researchers are encouraged to not only fine-tune strategies and pre-trained weights but also systematically investigate self-supervised learning techniques across various categories within their medical image datasets [39]. Additionally, testing newly developed strategies on multiple datasets, ideally encompassing diverse modalities and medical imaging domains, is recommended to foster a more comprehensive understanding of their potential and limitations.

7.1. Implementation Suggestion

Given the rapidly evolving nature and significant practical implications of medical image generation and translation, along with the increasing prominence of diffusion models, the pursuit of an optimal medical image generative model remains an ongoing challenge. In response, we have conducted a thorough survey and detailed comparative analysis of prior research. Our goal is to offer researchers a comprehensive set of implementation guidelines to support their exploration of methodologies in medical image generation and translation.

7.1.1. Unified Model or Specific Task Model?

The unified model refers to the use of the same network architecture to accomplish any medical image synthesis task [38,139,147]. Specific task model is designed to excel at a single task [160–162]. It is optimized specifically for that task, without considering other related tasks. Specific task models are often used when the task is complex or requires specialized features or architecture that may not be applicable to other tasks. While these models can achieve high performance for their specific task, they may not generalize well to other tasks.

 doi:10.20944/preprints202512.1407.v1

Given that only a subset of studies has undergone testing across multiple modalities, it is crucial to acknowledge that arriving at definitive conclusions regarding the most optimal generative model for medical image generation is not straightforward. Furthermore, the selection of the most suitable medical image generation model depends on a multitude of factors, including dataset dimensions, complexity, and the specific requirements imposed by various downstream tasks [17,34].

Within the scope of this comprehensive review, only a limited number of studies have rigorously evaluated their methodologies across multiple modalities and anatomical regions. In contrast, the majority of research efforts have concentrated on analyzing single modalities or specific anatomical areas. In practice, the significant differences among various modalities, as well as the substantial variations observed across different organs, tissues, and pathological conditions, present a considerable challenge. This challenge arises because a single, universal model would struggle to consistently outperform task-specific models across the diverse range of modalities and anatomical domains. Therefore, we recommend that researchers carefully tailor generative models to meet the unique requirements of various downstream tasks, image modalities, and anatomical or pathological contexts.

7.1.2. GAN or Diffusion Model?

Since debut in 2014, GANs have seen widespread adoption in the field of medical image synthesis. This popularity can be ascribed to GANs' utilization of adversarial learning strategy, which has consistently showcased superior generative capabilities in comparison to alternative image synthesis methods like VAEs and Flow-based models [279]. However, it's important to acknowledge that GANs frequently face challenges during their training process, and their stability relies on the careful selection of hyperparameters and regularization terms. Nonetheless, GANs maintain their prominent position within the domain of medical image synthesis [21].

In the year 2020, the landscape of image synthesis underwent a transformation with the advent of DDPM [280]. This novel framework exhibited remarkable image synthesis prowess, swiftly outperforming GANs in various aspects. Empirical research has provided compelling evidence that Diffusion models exhibit a heightened capacity to capture a broader spectrum of sample diversity compared to GANs [281]. While we strongly believe in the potential of diffusion models as a promising direction in generative modeling, it is important to note that their reliance on multiple denoising steps can result in a slower sampling process compared to the faster sampling capabilities of GANs. A promising approach to addressing this latency issue involves reducing sampling time while maintaining high image quality [282]. Subsequent research endeavors in this trajectory hold promise for narrowing the sampling speed disparity between diffusion models and GANs without compromising the fidelity of generated images.

Generative models confront a tripartite quandary, as elucidated by Kazerouni et al. [34]. While GANs excel at rapidly generating high-fidelity samples, their effectiveness is constrained by limited mode coverage. In contrast, VAEs and Normalizing Flows exhibit significant diversity in their samples but often at the expense of reduced sampling quality. Addressing these limitations, Diffusion models have emerged as a powerful solution, demonstrating the ability to achieve extensive mode coverage while maintaining high sample quality. However, it is important to recognize that the iterative nature of Diffusion models can lead to prolonged sampling times, making them computationally demanding and highlighting the need for further optimization [281].

In the domain of image creation tasks, both GANs and Diffusion models were initially applied to image generation. However, empirical evidence substantiates that the synthesis quality of Diffusion models distinctly outshines that of GANs [283]. Conversely, in the realm of image translation, recent advancements in GAN technology have solidified their position as the dominant choice over Diffusion models. Notably, there is currently no established baseline model based on Diffusion models that parallels the widely recognized Pix2Pix and CycleGAN frameworks. As a result, the efficacy of Diffusion models in image translation tasks remains unproven and requires further investigation.

 doi:10.20944/preprints202512.1407.v1

7.1.3. Translation with Prior Knowledge

Due to the significant differences in information content among medical images from various modalities—often being entirely distinct—the importance of incorporating prior knowledge into medical image generation tasks becomes clear. Integrating prior knowledge is a crucial step toward improving the quality, authenticity, and clinical relevance of the generated images. This incorporation serves multiple purposes, guiding the generative process and ensuring that the resulting images maintain anatomical accuracy and clinical utility [284,285].

One strategy in the integration of prior knowledge involves the design of custom loss functions, engineered specifically to impose constraints rooted in prior knowledge [162,258]. A tangible illustration of this entails the incorporation of penalties or regularization terms into the loss function. These augmentations serve to incentivize the generated images to closely adhere to known anatomical structures or established clinical guidelines.

Furthermore, a critical aspect of leveraging prior knowledge involves preprocessing the training data. This preprocessing aims to highlight or extract specific features or anatomical structures of interest. Techniques such as image segmentation, registration, and other image processing methods can be strategically applied to enhance the quality of the input dataset, thereby providing the model with more robust and informative data.

In the pursuit of fortifying the model's capacity to leverage prior knowledge, recourse to pre-trained models or knowledge derived from related medical imaging tasks is a valuable strategy. Transfer learning emerges as a potent technique, allowing the model to glean insights from prior knowledge encoded within models trained on analogous tasks or datasets.

7.1.4. Other Possible Optimization Strategies for Training

In addition to adversarial training, alternative optimization strategies such as gradient perturbation and knowledge distillation have been proposed to enhance model robustness [286,287]. Gradient perturbation techniques improve the robustness and generalization of generative models by introducing controlled noise during training [288]. This strategy strengthens the model's ability to adapt to unseen data and reduces overfitting to specific training distributions [289]. Knowledge distillation optimizes medical image synthesis by transferring knowledge from complex teacher models to lightweight student models [290]. It enhances the model's generalization across multiple tasks, enabling it to perform diverse medical image synthesis tasks such as denoising, super-resolution, and modality translation [291]. By leveraging the stable generative capabilities of the teacher model, knowledge distillation mitigates the instability issues commonly encountered during generative model training [292,293].

7.2. Limitations and Future Research

This review paper summarizes recent advancements in deep learning-based medical image synthesis methods. However, several limitations should be acknowledged. First, it was not feasible to aggregate or statistically compare the performance of different generative models due to the heterogeneity of the included studies. These studies employed diverse imaging modalities, reported varied evaluation metrics, and applied models to different downstream tasks, making direct comparisons challenging.

Second, our classification approach was unidimensional. In Section 5, we categorized studies based on downstream tasks, while in Section 6, we grouped them by target modality for image generation. This approach may not facilitate a comprehensive comparative analysis of generative model methods. Future reviews could adopt a more nuanced classification framework, such as categorizing studies by image generation techniques, which might provide deeper insights into the strengths and weaknesses of different synthesis methods.

Third, while diffusion models have rapidly advanced in natural image generation since 2022 [283] and are increasingly being applied to medical image synthesis [34], most relevant papers are

 doi:10.20944/preprints202512.1407.v1

currently in preprint form. Due to the absence of peer review, these preprints were excluded from this review, resulting in limited coverage of diffusion models. As these models gain traction in medical image synthesis, future reviews should incorporate peer-reviewed studies to provide a more comprehensive assessment.

The study selection process may also have introduced biases. Reliance on specific databases and keywords might have excluded relevant studies from other sources, such as conference proceedings and technical reports. Additionally, the focus on English-language literature and timeframe restrictions may have led to the omission of significant non-English studies or earlier research. These limitations highlight the need for broader search strategies in future reviews.

Regarding gaps in the literature, several underexplored areas were identified. For instance, the application of physics-based generative models in medical image synthesis has received limited attention. Similarly, research on the generalizability of generative models across different disease stages or imaging devices remains scarce. Addressing these gaps could enhance the comprehensiveness of future assessments.

Finally, several challenges were encountered during the review process. Standardizing data extraction was difficult due to variations in metrics and reporting methods across studies, which hindered direct comparisons. The heterogeneity of studies—such as differences in dataset size, quality, and evaluation metrics—further complicated the synthesis of findings. Additionally, insufficient methodological detail in some studies made it challenging to fully interpret their results and methodologies. These challenges underscore the need for more standardized reporting practices in future research.

8. Conclusions

Medical image synthesis based on deep learning is an emerging and rapidly growing field. In this review, we categorize medical image synthesis into two main types: creation and translation. Creation focuses on generating new images from potential conditional variables, while translation involves mapping images from one or more modalities to another, preserving semantic and informational content.

Currently, medical image synthesis based on deep learning primarily utilizes three models: VAE, GANs, and Diffusion models. Each of these models has distinct characteristics, and the choice among them depends on the specific requirements of the task. The diffusion model, in particular, has demonstrated outstanding performance in natural image generation, earning widespread recognition. It is reasonable to anticipate that future research will increasingly focus on medical image creation and translation using diffusion models. Exploring methods to reduce the training and inference time of diffusion models while maintaining high generation quality may represent a promising research direction in the years to come.

Through an analysis of the literature included in this review, it is evident that deep learning-based medical image creation is a powerful technique for enhancing the performance of downstream tasks. It addresses data limitations, improves generalization, reduces overfitting, and increases model robustness to diverse imaging conditions and variations. Modality translation, on the other hand, can supplement missing modalities, aiding in diagnosis and enhancing downstream tasks such as attenuation correction for PET/MRI, radiotherapy planning without CT images, and CBCT denoising. Additionally, translation between contrast-enhanced and non-contrast images primarily aims to reduce costs, both in terms of time and financial resources, while also offering the potential for more accurate diagnoses, particularly for patients with kidney diseases. Overall, medical image translation based on generative models is multifaceted, highly effective, and holds significant promise for the future.

Author Contributions: HP and TZ conducted the literature search and analysis and drafted the work. YW and SC made substantial contribution to the interpretation of data and literatures. WQ, YY, CY, PM and SQ designed

 doi:10.20944/preprints202512.1407.v1

the work and made major contributions in writing the manuscript. All authors read and approved the final manuscript.

Funding: This work was partly supported by the National Natural Science Foundation of China under Grant (Nos. 82472076, 62271131), and the Fundamental Research Funds for the Central Universities (N25BJD013).

Institutional Review Board Statement: Not applicable.

Informed Consent Statement: Not applicable.

Data Availability Statement: Data sharing is not applicable to this article as no datasets were generated or analysed during the current study.

Acknowledgments: Not applicable.

Conflicts of Interest: The authors declare that they have no competing interests.

List of Abbreviations

CBCT	Cone Beam Computed Tomography	MRA	Magnetic Resonance Angiography
CT	Computed Tomography	MRI	Magnetic Resonance Imaging
DM	Diffusion Model	PD	Proton density image
DWI	Diffusion-Weighted Image	PET	Positron Emission Tomography
FID	Fréchet Inception Distance	PSNR	Peak Signal-to-Noise Ratio
FLAIR	Fluid-Attenuated Inversion Recovery	RMSE	Root Mean Square Error
GAN	Generative Adversarial Network	SSIM	Structural Similarity Index
IS	Inception Score	T1w	T1-weighted image
MAE	Mean Absolute Error	T2w	T2-weighted image
MMD	Maximum Mean Discrepancy	US	Ultrasound imaging
MS	Mode Score	VAE	Variational Autoencoder
MSE	Mean Square Error	WD	Wasserstein distance

References

1. X. Chen, X. Wang, K. Zhang, K.-M. Fung, T.C. Thai, K. Moore, R.S. Mannel, H. Liu, B. Zheng, Y.J.M.i.a. Qiu, Recent advances and clinical applications of deep learning in medical image analysis, Medical image analysis, 79 (2022) 102444.
2. Y. Zhou, M.A. Chia, S.K. Wagner, M.S. Ayhan, D.J. Williamson, R.R. Struyven, T. Liu, M. Xu, M.G. Lozano, P.J.N. Woodward-Court, A foundation model for generalizable disease detection from retinal images, Nature, 622 (2023) 156-163.
3. J. Ma, Y. He, F. Li, L. Han, C. You, B.J.N.C. Wang, Segment anything in medical images, Nature Communications, 15 (2024) 654.
4. K. Cao, Y. Xia, J. Yao, X. Han, L. Lambert, T. Zhang, W. Tang, G. Jin, H. Jiang, X.J.N.m. Fang, Large-scale pancreatic cancer detection via non-contrast CT and deep learning, Nature Medicine, 29 (2023) 3033-3043.
5. C. Liu, Z. Zhuo, L. Qu, Y. Jin, T. Hua, J. Xu, G. Tan, Y. Li, Y. Duan, T.J.S.b. Wang, DeepWMH: A deep learning tool for accurate white matter hyperintensity segmentation without requiring manual annotations for training, Science Bulletin, (2024) S2095-9273 (2024) 00061-00066.
6. Q. Lu, W. Liu, Z. Zhuo, Y. Li, Y. Duan, P. Yu, L. Qu, C. Ye, Y.J.M.I.A. Liu, A transfer learning approach to few-shot segmentation of novel white matter tracts, Medical Image Analysis, 79 (2022) 102454.
7. W. Liu, Z. Zhuo, Y. Liu, C.J.M.I.A. Ye, One-shot segmentation of novel white matter tracts via extensive data augmentation and adaptive knowledge transfer, Medical Image Analysis, 90 (2023) 102968.
8. S. Vellmer, M. Tabelow, H. Zhang, Diffusion MRI GAN Synthesizing Fibre Orientation Distributions for White Matter Simulation, Communications Biology, 8 (2025) 7936. https://doi.org/10.1038/s42003-025-07936-w.
9. G. Schuit, D. Parra, C. Besa, Perceptual Evaluation of GANs and Diffusion Models for Generating X-rays, arXiv preprint arXiv:2508.07128 (2025).

 doi:10.20944/preprints202512.1407.v1

10. O.O. Ejiga, M. Anifowose, L. Yuan, Advancing AI-Powered Medical Image Synthesis: Insights from the MedVQA-GI Challenge, arXiv preprint arXiv:2502.20667 (2025).
11. Z. Yang, Y. Li, W. Wang, seg2med: A Segmentation-based Medical Image Generation Framework Using Denoising Diffusion Probabilistic Models, arXiv preprint arXiv:2504.09182 (2025)
12. C. Zhao, P. Guo, Y. Xu, MAISI-v2: Accelerated 3D High-Resolution Medical Image Synthesis with Rectified Flow and Region-specific Contrastive Loss, arXiv preprint arXiv:2508.05772 (2025).
13. J. Kim, S. Lee, FMed-Diffusion: Federated Learning on Medical Image Diffusion Models for Privacy-Preserving Data Generation, bioRxiv preprint (2025)
14. T. Chakraborty, S.M. Naik, M. Panja, B. Manvitha, Ten Years of Generative Adversarial Nets (GANs): A survey of the state-of-the-art, arXiv preprint arXiv:2308.16316, (2023).
15. E. Goceri, Medical image data augmentation: techniques, comparisons and interpretations, Artificial Intelligence Review, (2023) 1-45.
16. A. Kebaili, J. Lapuyade-Lahorgue, S. Ruan, Deep Learning Approaches for Data Augmentation in Medical Imaging: A Review, Journal of Imaging, 9 (2023) 81.
17. S. Dayarathna, K.T. Islam, S. Uribe, G. Yang, M. Hayat, Z. Chen, Deep learning based synthesis of MRI, CT and PET: Review and analysis, Medical Image Analysis, (2023) 103046.
18. T.H. Wang, Y. Lei, Y.B. Fu, J.F. Wynne, W.J. Curran, T. Liu, X.F. Yang, A review on medical imaging synthesis using deep learning and its clinical applications, Journal of Applied Clinical Medical Physics, 22 (2021) 11-36.
19. X. Yi, E. Walia, P. Babyn, Generative adversarial network in medical imaging: A review, Medical Image Analysis, 58 (2019).
20. S. Kazeminia, C. Baur, A. Kuijper, B. van Ginneken, N. Navab, S. Albarqouni, A. Mukhopadhyay, GANs for medical image analysis, Artificial Intelligence in Medicine, 109 (2020) 101938.
21. Y.Z. Chen, X.H. Yang, Z.H. Wei, A.A. Heidari, N.G. Zheng, Z.C. Li, H.L. Chen, H.G. Hu, Q.W. Zhou, Q. Guan, Generative Adversarial Networks in Medical Image augmentation: A review, Computers in Biology and Medicine, 144 (2022).
22. R. Osuala, K. Kushibar, L. Garrucho, A. Linardos, Z. Szafranowska, S. Klein, B. Glocker, O. Diaz, K. Lekadir, Data synthesis and adversarial networks: A review and meta-analysis in cancer imaging, Medical Image Analysis, (2022) 102704.
23. J. Zhao, X.Y. Hou, M.Q. Pan, H. Zhang, Attention-based generative adversarial network in medical imaging: A narrative review, Computers in Biology and Medicine, 149 (2022).
24. A.F. Frangi, S.A. Tsaftaris, J.L. Prince, Simulation and Synthesis in Medical Imaging, Ieee Transactions on Medical Imaging, 37 (2018) 673-679.
25. A. Oussidi, A. Elhassouny, Deep generative models: Survey, 2018 International conference on intelligent systems and computer vision (ISCV), IEEE, 2018, pp. 1-8.
26. D.P. Kingma, M. Welling, Auto-encoding variational bayes, arXiv preprint arXiv:1312.6114, (2013).
27. T. Salimans, D. Kingma, M. Welling, Markov chain monte carlo and variational inference: Bridging the gap, International conference on machine learning, PMLR, 2015, pp. 1218-1226.
28. T.D. Kulkarni, W.F. Whitney, P. Kohli, J. Tenenbaum, Deep convolutional inverse graphics network, Advances in neural information processing systems, 28 (2015).
29. K. Gregor, I. Danihelka, A. Graves, D. Rezende, D. Wierstra, Draw: A recurrent neural network for image generation, International conference on machine learning, PMLR, 2015, pp. 1462-1471.
30. M. Pesteie, P. Abolmaesumi, R.N. Rohling, Adaptive augmentation of medical data using independently conditional variational auto-encoders, IEEE transactions on medical imaging, 38 (2019) 2807-2820.
31. L.Y.H. Alex, J. Galeotti, Ultrasound Variational Style Transfer to Generate Images Beyond the Observed Domain, 1st Workshop on Deep Generative Models for Medical Image Computing and Computer Assisted Intervention (DGM4MICCAI) / 1st MICCAI Workshop on Data Augmentation, Labelling, and Imperfections (DALI)Electr Network, 2021, pp. 14-23.
32. R. Wei, A. Mahmood, Recent advances in variational autoencoders with representation learning for biomedical informatics: A survey, Ieee Access, 9 (2020) 4939-4956.

 doi:10.20944/preprints202512.1407.v1

33. I. Goodfellow, J. Pouget-Abadie, M. Mirza, B. Xu, D. Warde-Farley, S. Ozair, A. Courville, Y. Bengio, Generative adversarial networks, Communications of the ACM, 63 (2020) 139-144.
34. A. Kazerouni, E.K. Aghdam, M. Heidari, R. Azad, M. Fayyaz, I. Hacihaliloglu, D. Merhof, Diffusion models in medical imaging: A comprehensive survey, Medical Image Analysis, (2023) 102846.
35. P. Isola, J.-Y. Zhu, T. Zhou, A.A. Efros, Image-to-image translation with conditional adversarial networks, Proceedings of the IEEE conference on computer vision and pattern recognition, 2017, pp. 1125-1134.
36. J.-Y. Zhu, T. Park, P. Isola, A.A. Efros, Unpaired image-to-image translation using cycle-consistent adversarial networks, Proceedings of the IEEE international conference on computer vision, 2017, pp. 2223-2232.
37. B. Sun, S.F. Jia, X.L. Jiang, F.C. Jia, Double U-Net CycleGAN for 3D MR to CT image synthesis, International Journal of Computer Assisted Radiology and Surgery, (2023).
38. S.U.H. Dar, M. Yurt, L. Karacan, A. Erdem, E. Erdem, T. Cukur, Image Synthesis in Multi-Contrast MRI With Conditional Generative Adversarial Networks, Ieee Transactions on Medical Imaging, 38 (2019) 2375-2388.
39. H. Pang, S. Qi, Y. Wu, M. Wang, C. Li, Y. Sun, W. Qian, G. Tang, J. Xu, Z. Liang, NCCT-CECT image synthesizers and their application to pulmonary vessel segmentation, Computer Methods and Programs in Biomedicine, 231 (2023) 107389.
40. S. Pan, T. Wang, R.L. Qiu, M. Axente, C.-W. Chang, J. Peng, A.B. Patel, J. Shelton, S.A. Patel, J. Roper, 2D medical image synthesis using transformer-based denoising diffusion probabilistic model, Physics in Medicine & Biology, 68 (2023) 105004.
41. Z. Dorjsembe, S. Odonchimed, F. Xiao, Three-dimensional medical image synthesis with denoising diffusion probabilistic models, Medical Imaging with Deep Learning, 2022.
42. M. Özbey, O. Dalmaz, S.U. Dar, H.A. Bedel, Ş. Özturk, A. Güngör, T. Çukur, Unsupervised medical image translation with adversarial diffusion models, IEEE Transactions on Medical Imaging, (2023).
43. Z.-X. Cui, C. Cao, S. Liu, Q. Zhu, J. Cheng, H. Wang, Y. Zhu, D. Liang, Self-score: Self-supervised learning on score-based models for mri reconstruction, arXiv preprint arXiv:2209.00835, (2022).
44. C. Peng, P. Guo, S.K. Zhou, V.M. Patel, R. Chellappa, Towards performant and reliable undersampled MR reconstruction via diffusion model sampling, International Conference on Medical Image Computing and Computer-Assisted Intervention, Springer, 2022, pp. 623-633.
45. D. Hu, Y.K. Tao, I. Oguz, Unsupervised denoising of retinal OCT with diffusion probabilistic model, Medical Imaging 2022: Image Processing, SPIE, 2022, pp. 25-34.
46. B. Kim, I. Han, J.C. Ye, DiffuseMorph: unsupervised deformable image registration using diffusion model, European Conference on Computer Vision, Springer, 2022, pp. 347-364.
47. Y. Yang, H. Fu, A. Aviles-Rivero, C.-B. Schönlieb, L. Zhu, DiffMIC: Dual-Guidance Diffusion Network for Medical Image Classification, arXiv preprint arXiv:2303.10610, (2023).
48. A. Rahman, J.M.J. Valanarasu, I. Hacihaliloglu, V.M. Patel, Ambiguous medical image segmentation using diffusion models, Proceedings of the IEEE/CVF Conference on Computer Vision and Pattern Recognition, 2023, pp. 11536-11546.
49. J. Wolleb, R. Sandkühler, F. Bieder, P. Valmaggia, P.C. Cattin, Diffusion models for implicit image segmentation ensembles, International Conference on Medical Imaging with Deep Learning, PMLR, 2022, pp. 1336-1348.
50. S.-C. Huang, A. Pareek, M. Jensen, M.P. Lungren, S. Yeung, A.S. Chaudhari, Self-supervised learning for medical image classification: a systematic review and implementation guidelines, NPJ Digital Medicine, 6 (2023) 74.
51. A. Obukhov, M. Krasnyanskiy, Quality assessment method for GAN based on modified metrics inception score and Fréchet inception distance, Software Engineering Perspectives in Intelligent Systems: Proceedings of 4th Computational Methods in Systems and Software 2020, Vol. 1 4, Springer, 2020, pp. 102-114.
52. E. Miranda, M. Aryuni, E. Irwansyah, A survey of medical image classification techniques, 2016 international conference on information management and technology (ICIMTech), IEEE, 2016, pp. 56-61.

 doi:10.20944/preprints202512.1407.v1

53. L. Gao, L. Zhang, C. Liu, S.J.A.i.i.m. Wu, Handling imbalanced medical image data: A deep-learning-based one-class classification approach, 108 (2020) 101935.
54. H. Salehinejad, E. Colak, T. Dowdell, J. Barfett, S. Valaee, Synthesizing Chest X-Ray Pathology for Training Deep Convolutional Neural Networks, Ieee Transactions on Medical Imaging, 38 (2019) 1197-1206.
55. S.Y. Pan, T.H. Wang, R.L.J. Qiu, M. Axente, C.W. Chang, J.B. Peng, A.B. Patel, J. Shelton, S.A. Patel, J. Roper, X.F. Yang, 2D medical image synthesis using transformer-based denoising diffusion probabilistic model, Physics in Medicine and Biology, 68 (2023).
56. P. Chlap, H. Min, N. Vandenberg, J. Dowling, L. Holloway, A.J.J.o.M.I. Haworth, R. Oncology, A review of medical image data augmentation techniques for deep learning applications, 65 (2021) 545-563.
57. G.A. Kaissis, M.R. Makowski, D. Rückert, R.F.J.N.M.I. Braren, Secure, privacy-preserving and federated machine learning in medical imaging, 2 (2020) 305-311.
58. R. Wang, T. Lei, R. Cui, B. Zhang, H. Meng, A.K.J.I.I.P. Nandi, Medical image segmentation using deep learning: A survey, 16 (2022) 1243-1267.
59. P.F. Guo, P.Y. Wang, R. Yasarla, J.Y. Zhou, V.M. Patel, S.S. Jiang, Anatomic and Molecular MR Image Synthesis Using Confidence Guided CNNs, Ieee Transactions on Medical Imaging, 40 (2021) 2832-2844.
60. J. Zhang, L.D. Yu, D.C. Chen, W.D. Pan, C. Shi, Y. Niu, X.W. Yao, X.B. Xu, Y. Cheng, Dense GAN and multi-layer attention based lesion segmentation method for COVID-19 CT images, Biomedical Signal Processing and Control, 69 (2021).
61. S. Amirrajab, C. Lorenz, J. Weese, J. Pluim, M. Breeuwer, Pathology Synthesis of 3D Consistent Cardiac MR Images Using 2D VAEs and GANs, 7th International Workshop on Simulation and Synthesis in Medical Imaging (SASHIMI)Singapore, SINGAPORE, 2022, pp. 34-42.
62. C. Han, Y. Kitamura, A. Kudo, A. Ichinose, L. Rundo, Y. Furukawa, K. Umemoto, Y.Z. Li, H. Nakayama, I.C. Soc, Synthesizing Diverse Lung Nodules Wherever Massively: 3D Multi-Conditional GAN-based CT Image Augmentation for Object Detection, 7th International Conference on 3D Vision (3DV)Quebec City, CANADA, 2019, pp. 729-737.
63. A. Kamli, R. Saouli, H. Batatia, M.B. Ben Naceur, I. Youkana, Synthetic medical image generator for data augmentation and anonymisation based on generative adversarial network for glioblastoma tumors growth prediction, Iet Image Processing, 14 (2020) 4248-4257.
64. Z.Y. Li, Q.Y. Fan, B. Bilgic, G.Z. Wang, W.C. Wu, J.R. Polimeni, K.L. Miller, S.Y. Huang, Q.Y. Tian, Diffusion MRI data analysis assisted by deep learning synthesized anatomical images (DeepAnat), Medical Image Analysis, 86 (2023).
65. M. Frid-Adar, I. Diamant, E. Klang, M. Amitai, J. Goldberger, H. Greenspan, GAN-based synthetic medical image augmentation for increased CNN performance in liver lesion classification, Neurocomputing, 321 (2018) 321-331.
66. Q.Q. Zhang, H.F. Wang, H.Y. Lu, D. Won, S.W. Yoon, I.C. Soc, Medical Image Synthesis with Generative Adversarial Networks for Tissue Recognition, 6th IEEE International Conference on Healthcare Informatics (ICHI)New York, NY, 2018, pp. 199-207.
67. Y.J. Lin, I.F. Chung, Ieee, Medical Data Augmentation Using Generative Adversarial Networks X-ray Image Generation for Transfer Learning of Hip Fracture Detection, International Conference on Technologies and Applications of Artficial Intelligence (TAAI)Kaohsiung, TAIWAN, 2019.
68. J. Yang, S.Q. Liu, S. Grbic, A.A.A. Setio, Z.B. Xu, E. Gibson, G. Chabin, B. Georgescu, A.F. Laine, D. Comaniciu, Ieee, CLASS-AWARE ADVERSARIAL LUNG NODULE SYNTHESIS IN CT IMAGES, 16th IEEE International Symposium on Biomedical Imaging (ISBI)Venice, ITALY, 2019, pp. 1348-1352.
69. R.Z.J. Choong, S.A. Harding, B.Y. Tang, S.W. Liao, Ieee, 3-To-1 Pipeline: Restructuring Transfer Learning Pipelines for Medical Imaging Classification via Optimized GAN Synthetic Images, 42nd Annual International Conference of the IEEE-Engineering-in-Medicine-and-Biology-Society (EMBC)Montreal, CANADA, 2020, pp. 1596-1599.
70. S. Menon, J. Galita, D. Chapman, A. Gangopadhyay, J. Mangalagiri, P. Nguyen, Y. Yesha, Y. Yesha, B. Saboury, M. Morris, Generating Realistic COVID-19 x-rays with a Mean Teacher plus Transfer Learning GAN, 8th IEEE International Conference on Big Data (Big Data)Electr Network, 2020, pp. 1216-1225.

 doi:10.20944/preprints202512.1407.v1

71. P. Ahmad, Y. Wang, M. Havaei, CT-SGAN: Computed Tomography Synthesis GAN, 1st Workshop on Deep Generative Models for Medical Image Computing and Computer Assisted Intervention (DGM4MICCAI) / 1st MICCAI Workshop on Data Augmentation, Labelling, and Imperfections (DALI)Electr Network, 2021, pp. 67-79.
72. A.A.E. Ambita, E.N.V. Boquio, P.C. Naval, COViT-GAN: Vision Transformer for COVID-19 Detection in CT Scan Images with Self-Attention GAN for Data Augmentation, 30th International Conference on Artificial Neural Networks (ICANN)Electr Network, 2021, pp. 587-598.
73. H. Che, S. Ramanathan, D.J. Foran, J.L. Nosher, V.M. Patel, I. Hacihaliloglu, Realistic Ultrasound Image Synthesis for Improved Classification of Liver Disease, 2nd International Workshop on Advances in Simplifying Medical UltraSound (ASMUS)Electr Network, 2021, pp. 179-188.
74. T. Pang, J.H.D. Wong, W.L. Ng, C.S. Chan, Semi-supervise d GAN-base d Radiomics Model for Data Augmentation in Breast Ultrasound Mass Classification, Computer Methods and Programs in Biomedicine, 203 (2021).
75. R. Toda, A. Teramoto, M. Tsujimoto, H. Toyama, K. Imaizumi, K. Saito, H. Fujita, Synthetic CT image generation of shape-controlled lung cancer using semi-conditional InfoGAN and its applicability for type classification, International Journal of Computer Assisted Radiology and Surgery, 16 (2021) 241-251.
76. S.K. Venu, Improving the Generalization of Deep Learning Classification Models in Medical Imaging Using Transfer Learning and Generative Adversarial Networks, 13th International Conference on Agents and Artificial Intelligence (ICAART)Electr Network, 2021, pp. 218-235.
77. G.Y. Zhang, K.X. Chen, S.L. Xu, P.C.A. Cho, Y. Nan, X. Zhou, C.A.F. Lv, C.S. Li, G.T. Xie, Lesion synthesis to improve intracranial hemorrhage detection and classification for CT images, Computerized Medical Imaging and Graphics, 90 (2021).
78. R.N. Abirami, P. Vincent, V. Rajinikanth, S. Kadry, COVID-19 Classification Using Medical Image Synthesis by Generative Adversarial Networks, International Journal of Uncertainty Fuzziness and Knowledge-Based Systems, 30 (2022) 385-401.
79. A. Fernandez-Quilez, O. Parvez, T. Eftestol, S.R. Kjosavik, K. Oppedal, Improving prostate cancer triage with GAN-based synthetically generated prostate ADC MRI, Conference on Medical Imaging - Computer-Aided DiagnosisElectr Network, 2022.
80. Q. Guan, Y.Z. Chen, Z.H. Wei, A.A. Heidari, H.G. Hu, X.H. Yang, J.W. Zheng, Q.W. Zhou, H.L. Chen, F. Chen, Medical image augmentation for lesion detection using a texture-constrained multichannel progressive GAN, Computers in Biology and Medicine, 145 (2022).
81. Z. Liang, J.X. Huang, S. Antani, Image translation by Ad cycleGAN for COVID-19 X-ray images: A new approach for controllable GAN, Sensors, 22 (2022) 9628.
82. J.W. Mao, X.S. Yin, G.D. Zhang, B.W. Chen, Y.Q. Chang, W.B. Chen, J.Y. Yu, Y.G. Wang, Pseudo-labeling generative adversarial networks for medical image classification, Computers in Biology and Medicine, 147 (2022).
83. D.I. Moris, J. de Moura, J. Novo, M. Ortega, Unsupervised contrastive unpaired image generation approach for improving tuberculosis screening using chest X-ray images, Pattern Recognition Letters, 164 (2022) 60-66.
84. E. Ovalle-Magallanes, J.G. Avina-Cervantes, I. Cruz-Aceves, J. Ruiz-Pinales, Improving convolutional neural network learning based on a hierarchical bezier generative model for stenosis detection in X-ray images, Computer Methods and Programs in Biomedicine, 219 (2022).
85. P.M. Shah, H. Ullah, R. Ullah, D. Shah, Y.L. Wang, S. ul Islam, A. Gani, J. Rodrigues, DC-GAN-based synthetic X-ray images augmentation for increasing the performance of EfficientNet for COVID-19 detection, Expert Systems, 39 (2022).
86. Y.F. Chen, Y.L. Lin, X.D. Xu, J.Z. Ding, C.Z. Li, Y.M. Zeng, W.F. Xie, J.L. Huang, Multi-domain medical image translation generation for lung image classification based on generative adversarial networks, Computer Methods and Programs in Biomedicine, 229 (2023).
87. Y. Kim, J.H. Lee, C. Kim, K.N. Jin, C.M. Park, GAN based ROI conditioned Synthesis of Medical Image for Data Augmentation, Conference on Medical Imaging - Image ProcessingSan Diego, CA, 2023.

 doi:10.20944/preprints202512.1407.v1

88. A. Wali, M. Ahmad, A. Naseer, M. Tamoor, S.A.M. Gilani, StynMedGAN: Medical images augmentation using a new GAN model for improved diagnosis of diseases, Journal of Intelligent & Fuzzy Systems, 44 (2023) 10027-10044.
89. F. Tom, D. Sheet, Ieee, SIMULATING PATHO-REALISTIC ULTRASOUND IMAGES USING DEEP GENERATIVE NETWORKS WITH ADVERSARIAL LEARNING, 15th IEEE International Symposium on Biomedical Imaging (ISBI)Washington, DC, 2018, pp. 1174-1177.
90. L. Bargsten, A. Schlaefer, SpeckleGAN: a generative adversarial network with an adaptive speckle layer to augment limited training data for ultrasound image processing, International Journal of Computer Assisted Radiology and Surgery, 15 (2020) 1427-1436.
91. N.J. Cronin, T. Finni, O. Seynnes, Using deep learning to generate synthetic B-mode musculoskeletal ultrasound images, Computer Methods and Programs in Biomedicine, 196 (2020).
92. Y.L. Qu, W.Q. Su, X. Lv, C.F. Deng, Y. Wang, Y.T. Lu, Z.G. Chen, N. Xiao, Synthesis of Registered Multimodal Medical Images with Lesions, 29th International Conference on Artificial Neural Networks (ICANN)Bratislava, SLOVAKIA, 2020, pp. 774-786.
93. A. Zama, S.H. Park, H. Bang, C.W. Park, I. Park, S. Joung, Generative approach for data augmentation for deep learning-based bone surface segmentation from ultrasound images, International Journal of Computer Assisted Radiology and Surgery, 15 (2020) 931-941.
94. A. Fernandez-Quilez, S.V. Larsen, M. Goodwin, T.O. Gulsrud, S.R. Kjosavik, K. Oppedal, Ieee, IMPROVING PROSTATE WHOLE GLAND SEGMENTATION IN T2-WEIGHTED MRI WITH SYNTHETICALLY GENERATED DATA, 18th IEEE International Symposium on Biomedical Imaging (ISBI)Nice, FRANCE, 2021, pp. 1915-1919.
95. J.Z. Liang, J.Y. Chen, Ieee, Data Augmentation of Thyroid Ultrasound Images Using Generative Adversarial Network, IEEE International Ultrasonics Symposium (IEEE IUS)Electr Network, 2021.
96. S.Z. Yao, J.H. Tan, Y. Chen, Y.H. Gu, A weighted feature transfer gan for medical image synthesis, Machine Vision and Applications, 32 (2021).
97. J. Gao, W.H. Zhao, P. Li, W. Huang, Z.K. Chen, LEGAN: A Light and Effective Generative Adversarial Network for medical image synthesis, Computers in Biology and Medicine, 148 (2022).
98. J.M. Liang, X. Yang, Y.H. Huang, H.M. Li, S.C. He, X.D. Hu, Z.J. Chen, W.F. Xue, J. Cheng, D. Ni, Sketch guided and progressive growing GAN for realistic and editable ultrasound image synthesis, Medical Image Analysis, 79 (2022).
99. D. Lustermans, S. Amirrajab, M. Veta, M. Breeuwer, C.M. Scannell, Optimized automated cardiac MR scar quantification with GAN-based data augmentation, Computer Methods and Programs in Biomedicine, 226 (2022).
100. F. Lyu, M. Ye, A.J. Ma, T.C.F. Yip, G.L.H. Wong, P.C. Yuen, Learning From Synthetic CT Images via Test-Time Training for Liver Tumor Segmentation, Ieee Transactions on Medical Imaging, 41 (2022) 2510-2520.
101. M. Platscher, J. Zopes, C. Federau, Image translation for medical image generation: Ischemic stroke lesion segmentation, Biomedical Signal Processing and Control, 72 (2022).
102. S. Sasuga, A. Kudo, Y. Kitamura, S. Iizuka, E. Simo-Serra, A. Hamabe, M. Ishii, I. Takemasa, Image Synthesis-Based Late Stage Cancer Augmentation and Semi-supervised Segmentation for MRI Rectal Cancer Staging, 2nd MICCAI International Workshop on Data Augmentation, Labeling, and Imperfections (DALI)Singapore, SINGAPORE, 2022, pp. 1-10.
103. S. Shabani, M. Homayounfar, V. Vardhanabhuti, M.A.N. Mahani, M. Koohi-Moghadam, Self-supervised region-aware segmentation of COVID-19 CT images using 3D GAN and contrastive learning, Computers in Biology and Medicine, 149 (2022).
104. I. Sirazitdinov, H. Schulz, A. Saalbach, S. Renisch, D.V. Dylov, Tubular shape aware data generation for segmentation in medical imaging, International Journal of Computer Assisted Radiology and Surgery, 17 (2022) 1091-1099.
105. D. Tomar, B. Bozorgtabar, M. Lortkipanidze, G. Vray, M.S. Rad, J.P. Thiran, I.C. Soc, Self-Supervised Generative Style Transfer for One-Shot Medical Image Segmentation, 22nd IEEE/CVF Winter Conference on Applications of Computer Vision (WACV)Waikoloa, HI, 2022, pp. 1737-1747.

 doi:10.20944/preprints202512.1407.v1

106. A. Beji, A.G. Blaiech, M. Said, A. Ben Abdallah, M.H. Bedoui, An innovative medical image synthesis based on dual GAN deep neural networks for improved segmentation quality, Applied Intelligence, 53 (2023) 3381-3397.
107. J. Mendes, T. Pereira, F. Silva, J. Frade, J. Morgado, C. Freitas, E. Negrao, B.F. de Lima, M.C. da Silva, A.J. Madureira, I. Ramos, J.L. Costa, V. Hespanhol, A. Cunha, H.P. Oliveira, Lung CT image synthesis using GANs, Expert Systems with Applications, 215 (2023).
108. Z.R. Shen, X. Ouyang, B. Xiao, J.Z. Cheng, D.G. Shen, Q. Wang, Image synthesis with disentangled attributes for chest X-ray nodule augmentation and detection, Medical Image Analysis, 84 (2023).
109. X. Xing, G. Papanastasiou, S. Walsh, G. Yang, Less is More: Unsupervised Mask-guided Annotated CT Image Synthesis with Minimum Manual Segmentations, IEEE Transactions on Medical Imaging, (2023).
110. Y.P. Zhang, Q. Wang, B.L. Hu, MinimalGAN: diverse medical image synthesis for data augmentation using minimal training data, Applied Intelligence, (2023).
111. C. Han, H. Hayashi, L. Rundo, R. Araki, W. Shimoda, S. Muramatsu, Y. Furukawa, G. Mauri, H. Nakayama, Ieee, GAN-BASED SYNTHETIC BRAIN MR IMAGE GENERATION, 15th IEEE International Symposium on Biomedical Imaging (ISBI)Washington, DC, 2018, pp. 734-738.
112. L.H. Lee, J.A. Noble, Ieee, GENERATING CONTROLLABLE ULTRASOUND IMAGES OF THE FETAL HEAD, IEEE 17th International Symposium on Biomedical Imaging (ISBI)Iowa, IA, 2020, pp. 1761-1764.
113. Z.W. Wang, Y. Lin, K.T. Cheng, X. Yang, Semi-supervised mp-MRI data synthesis with StitchLayer and auxiliary distance maximization, Medical Image Analysis, 59 (2020).
114. J.A. Rodriguez-de-la-Cruz, H.G. Acosta-Mesa, E. Mezura-Montes, Ieee, Evolution of Generative Adversarial Networks Using PSO for Synthesis of COVID-19 Chest X-ray Images, IEEE Congress on Evolutionary Computation (IEEE CEC)Electr Network, 2021, pp. 2226-2233.
115. Z.R. Shen, X. Ouyang, Z.C. Wang, Y.Q. Zhan, Z. Xue, Q. Wang, J.Z. Cheng, D.G. Shen, Nodule Synthesis and Selection for Augmenting Chest X-ray Nodule Detection, 4th Chinese Conference on Pattern Recognition and Computer Vision (PRCV)Univ Sci & Technol Beijing, Zhuhai, PEOPLES R CHINA, 2021, pp. 536-547.
116. H. Sungmin, R. Marinescu, A.V. Dalca, A.K. Bonkhoff, M. Bretzner, N.S. Rost, P. Golland, 3D-StyleGAN: A Style-Based Generative Adversarial Network for Generative Modeling of Three-Dimensional Medical Images, 1st Workshop on Deep Generative Models for Medical Image Computing and Computer Assisted Intervention (DGM4MICCAI) / 1st MICCAI Workshop on Data Augmentation, Labelling, and Imperfections (DALI)Electr Network, 2021, pp. 24-34.
117. M.U. Kiru, B. Belaton, X. Chew, K.H. Almotairi, A.M. Hussein, M. Aminu, Comparative analysis of some selected generative adversarial network models for image augmentation: a case study of COVID-19 x-ray and CT images, Journal of Intelligent & Fuzzy Systems, 43 (2022) 7153-7172.
118. B. Cepa, C. Brito, A. Sousa, Ieee, Generative Adversarial Networks in Healthcare: A Case Study on MRI Image Generation, IEEE 7th Portuguese Meeting on Bioengineering (ENBENG)Porto, PORTUGAL, 2023, pp. 48-51.
119. L. Kong, C. Lian, D. Huang, Y. Hu, Q.J.A.i.N.I.P.S. Zhou, Breaking the dilemma of medical image-to-image translation, 34 (2021) 1964-1978.
120. J. Korhonen, J. You, Peak signal-to-noise ratio revisited: Is simple beautiful?, 2012 Fourth International Workshop on Quality of Multimedia Experience, IEEE, 2012, pp. 37-38.
121. D. Brunet, E.R. Vrscay, Z.J.I.T.o.I.P. Wang, On the mathematical properties of the structural similarity index, 21 (2011) 1488-1499.
122. A. Sharma, G. Hamarneh, Missing MRI Pulse Sequence Synthesis Using Multi-Modal Generative Adversarial Network, Ieee Transactions on Medical Imaging, 39 (2020) 1170-1183.
123. T. Zhou, H.Z. Fu, G. Chen, J.B. Shen, L. Shao, Hi-Net: Hybrid-Fusion Network for Multi-Modal MR Image Synthesis, Ieee Transactions on Medical Imaging, 39 (2020) 2772-2781.
124. J.Y. Wang, Q.M.J. Wu, F. Pourpanah, DC-cycleGAN: Bidirectional CT-to-MR synthesis from unpaired data, Computerized Medical Imaging and Graphics, 108 (2023).

 doi:10.20944/preprints202512.1407.v1

125. Y. Lei, T.H. Wang, S.B. Tian, X. Dong, A.B. Jani, D. Schuster, W.J. Curran, P. Patel, T. Liu, X.F. Yang, Male pelvic multi-organ segmentation aided by CBCT-based synthetic MRI, Physics in Medicine and Biology, 65 (2020).
126. F. Bazangani, F.J. Richard, B. Ghattas, E. Guedj, FDG-PET to T1 Weighted MRI Translation with 3D Elicit Generative Adversarial Network (E-GAN), Sensors, 22 (2022) 4640.
127. B.T. Yu, L.P. Zhou, L. Wang, J. Fripp, P. Bourgeat, Ieee, 3D CGAN BASED CROSS-MODALITY MR IMAGE SYNTHESIS FOR BRAIN TUMOR SEGMENTATION, 15th IEEE International Symposium on Biomedical Imaging (ISBI)Washington, DC, 2018, pp. 626-630.
128. B. Yu, L. Zhou, L. Wang, Y. Shi, J. Fripp, P. Bourgeat, Ea-GANs: edge-aware generative adversarial networks for cross-modality MR image synthesis, IEEE transactions on medical imaging, 38 (2019) 1750-1762.
129. B. Cao, H. Zhang, N.N. Wang, X.B. Gao, D.G. Shen, I. Assoc Advancement Artificial, Auto-GAN: Self-Supervised Collaborative Learning for Medical Image Synthesis, 34th AAAI Conference on Artificial Intelligence / 32nd Innovative Applications of Artificial Intelligence Conference / 10th AAAI Symposium on Educational Advances in Artificial IntelligenceNew York, NY, 2020, pp. 10486-10493.
130. A.Z.M. Shen, B.Y.F. Chen, C.K.S. Zhou, D.B. Georgescu, E.X.Q. Liu, F.T.S. Huang, Ieee, LEARNING A SELF-INVERSE NETWORK FOR BIDIRECTIONAL MRI IMAGE SYNTHESIS, IEEE 17th International Symposium on Biomedical Imaging (ISBI)Iowa, IA, 2020, pp. 1765-1769.
131. K. Wu, Y. Qiang, K. Song, X.T. Ren, W.K. Yang, W.J. Zhang, A. Hussain, Y.F. Cui, Image synthesis in contrast MRI based on super resolution reconstruction with multi-refinement cycle-consistent generative adversarial networks, Journal of Intelligent Manufacturing, 31 (2020) 1215-1228.
132. B.Y. Xin, Y.F. Hu, Y.F. Zheng, O.G. Liao, Ieee, MULTI-MODALITY GENERATIVE ADVERSARIAL NETWORKS WITH TUMOR CONSISTENCY LOSS FOR BRAIN MR IMAGE SYNTHESIS, IEEE 17th International Symposium on Biomedical Imaging (ISBI)Iowa, IA, 2020, pp. 1803-1807.
133. B.T. Yu, L.P. Zhou, L. Wang, Y.H. Shi, J. Fripp, P. Bourgeat, Sample-Adaptive GANs: Linking Global and Local Mappings for Cross-Modality MR Image Synthesis, Ieee Transactions on Medical Imaging, 39 (2020) 2339-2350.
134. M. Islam, N. Wijethilake, H.L. Ren, Glioblastoma multiforme prognosis: MRI missing modality generation, segmentation and radiogenomic survival prediction, Computerized Medical Imaging and Graphics, 91 (2021).
135. V. Kumar, M.K. Sharma, R. Jehadeesan, B. Venkatraman, G. Suman, A. Patra, A.H. Goenka, D. Sheet, Ieee, Learning to Generate Missing Pulse Sequence in MRI using Deep Convolution Neural Network Trained with Visual Turing Test, 43rd Annual International Conference of the IEEE-Engineering-in-Medicine-and-Biology-Society (IEEE EMBC)Electr Network, 2021, pp. 3419-3422.
136. Y.M. Luo, D. Nie, B. Zhan, Z.A. Li, X. Wu, J.L. Zhou, Y. Wang, D.G. Shen, Edge-preserving MRI image synthesis via adversarial network with iterative multi-scale fusion, Neurocomputing, 452 (2021) 63-77.
137. M.W. Ren, H. Kim, N. Dey, G. Gerig, Q-space Conditioned Translation Networks for Directional Synthesis of Diffusion Weighted Images from Multi-modal Structural MRI, International Conference on Medical Image Computing and Computer Assisted Intervention (MICCAI)Electr Network, 2021, pp. 530-540.
138. U. Upadhyay, V.P. Sudarshan, S.P. Awate, I.C. Soc, Uncertainty-aware GAN with Adaptive Loss for Robust MRI Image Enhancement, 18th IEEE/CVF International Conference on Computer Vision (ICCV)Electr Network, 2021, pp. 3248-3257.
139. C.J. Wang, G. Yang, G. Papanastasiou, S.A. Tsaftaris, D.E. Newby, C. Gray, G. Macnaught, T.J. MacGillivray, DiCyc: GAN-based deformation invariant cross-domain information fusion for medical image synthesis, Information Fusion, 67 (2021) 147-160.
140. K. Yan, Z.Z. Liu, S. Zheng, Z.Y. Guo, Z.F. Zhu, Y. Zhao, Coarse-to-Fine Learning Framework for Semi-supervised Multimodal MRI Synthesis, 6th Asian Conference on Pattern Recognition (ACPR)Electr Network, 2021, pp. 370-384.
141. H.R. Yang, J. Sun, L.W. Yang, Z.B. Xu, A Unified Hyper-GAN Model for Unpaired Multi-contrast MR Image Translation, International Conference on Medical Image Computing and Computer Assisted Intervention (MICCAI)Electr Network, 2021, pp. 127-137.

 doi:10.20944/preprints202512.1407.v1

142. M. Yurt, S.U.H. Dar, A. Erdem, E. Erdem, K.K. Oguz, T. Cukur, mustGAN: multi-stream Generative Adversarial Networks for MR Image Synthesis, Medical Image Analysis, 70 (2021).
143. B. Zhan, D. Li, Y. Wang, Z.Q. Ma, X. Wu, J.L. Zhou, L.P. Zhou, LR-cGAN: Latent representation based conditional generative adversarial network for multi-modality MRI synthesis, Biomedical Signal Processing and Control, 66 (2021).
144. T.X. Zhou, S. Canu, P. Vera, S. Ruan, Feature-enhanced generation and multi-modality fusion based deep neural network for brain tumor segmentation with missing MR modalities, Neurocomputing, 466 (2021) 102-112.
145. N.Y. Zhu, C. Liu, X.Y. Feng, D. Sikka, S. Gjerswold-Selleck, S.A. Small, J. Guo, I. Alzheimer's Dis Neuroimaging, Ieee, DEEP LEARNING IDENTIFIES NEUROIMAGING SIGNATURES OF ALZHEIMERiS DISEASE USING STRUCTURAL AND SYNTHESIZED FUNCTIONAL MRI DATA, 18th IEEE International Symposium on Biomedical Imaging (ISBI)Nice, FRANCE, 2021, pp. 216-220.
146. H.A. Amirkolaee, D.O. Bokov, H. Sharma, Development of a GAN architecture based on integrating global and local information for paired and unpaired medical image translation, Expert Systems with Applications, 203 (2022).
147. O. Dalmaz, M. Yurt, T. Cukur, ResViT: Residual Vision Transformers for Multimodal Medical Image Synthesis, Ieee Transactions on Medical Imaging, 41 (2022) 2598-2614.
148. P. Huang, D.W. Li, Z.C. Jiao, D.M. Wei, B. Cao, Z.H. Mo, Q. Wang, H. Zhang, D.G. Shen, Common feature learning for brain tumor MRI synthesis by context-aware generative adversarial network, Medical Image Analysis, 79 (2022).
149. J.X. Li, H.J. Chen, Y.F. Li, Y.H. Peng, J. Sun, P. Pan, Cross-modality synthesis aiding lung tumor segmentation on multi-modal MRI images, Biomedical Signal Processing and Control, 76 (2022).
150. Y. Lin, H. Han, S.K. Zhou, Ieee, DEEP NON-LINEAR EMBEDDING DEFORMATION NETWORK FOR CROSS-MODAL BRAIN MRI SYNTHESIS, 19th IEEE International Symposium on Biomedical Imaging (IEEE ISBI)Kolkata, INDIA, 2022.
151. L.M. Xu, H. Zhang, L.Y. Song, Y.R. Lei, Bi-MGAN: Bidirectional T1-to-T2 MRI images prediction using multi-generative multi-adversarial nets, Biomedical Signal Processing and Control, 78 (2022).
152. M. Yurt, M. Ozbey, S.U.H. Dar, B. Tinaz, K.K. Oguz, T. Cukur, Progressively volumetrized deep generative models for data-efficient contextual learning of MR image recovery, Medical Image Analysis, 78 (2022).
153. B. Zhan, L. Zhou, Z. Li, X. Wu, Y. Pu, J. Zhou, Y. Wang, D. Shen, D2FE-GAN: Decoupled dual feature extraction based GAN for MRI image synthesis, Knowledge-Based Systems, 252 (2022) 109362.
154. X.Z. Zhang, X.Z. He, J. Guo, N. Ettehadi, N. Aw, D. Semanek, J. Posner, A. Laine, Y. Wang, PTNet3D: A 3D High-Resolution Longitudinal Infant Brain MRI Synthesizer Based on Transformers, Ieee Transactions on Medical Imaging, 41 (2022) 2925-2940.
155. L. Zhu, Q. He, Y. Huang, Z.H. Zhang, J.M. Zeng, L. Lu, W.M. Kong, F.Q. Zhou, DualMMP-GAN: Dual-scale multi-modality perceptual generative adversarial network for medical image segmentation, Computers in Biology and Medicine, 144 (2022).
156. B. Cao, Z.W. Bi, Q.H. Hu, H. Zhang, N.N. Wang, X.B. Gao, D.G. Shen, AutoEncoder-Driven Multimodal Collaborative Learning for Medical Image Synthesis, International Journal of Computer Vision, 131 (2023) 1995-2014.
157. D. Kawahara, H. Yoshimura, T. Matsuura, A. Saito, Y. Nagata, MRI image synthesis for fluid-attenuated inversion recovery and diffusion-weighted images with deep learning, Physical and Engineering Sciences in Medicine, (2023).
158. J. Liu, S. Pasumarthi, B. Duffy, E. Gong, K. Datta, G. Zaharchuk, One model to synthesize them all: Multi-contrast multi-scale transformer for missing data imputation, IEEE Transactions on Medical Imaging, (2023).
159. R. Touati, S. Kadoury, A least square generative network based on invariant contrastive feature pair learning for multimodal MR image synthesis, International Journal of Computer Assisted Radiology and Surgery, 18 (2023) 971-979.
160. R. Touati, S. Kadoury, Bidirectional feature matching based on deep pairwise contrastive learning for multiparametric MRI image synthesis, Physics in Medicine and Biology, 68 (2023).

 doi:10.20944/preprints202512.1407.v1

161. B. Wang, Y. Pan, S. Xu, Y. Zhang, Y. Ming, L. Chen, X. Liu, C. Wang, Y. Liu, Y. Xia, Quantitative Cerebral Blood Volume Image Synthesis from Standard MRI Using Image-to-Image Translation for Brain Tumors, Radiology, 308 (2023) e222471.
162. Z.Q. Yu, X.Y. Han, S.J. Zhang, J.F. Feng, T.Y. Peng, X.Y. Zhang, MouseGAN plus plus : Unsupervised Disentanglement and Contrastive Representation for Multiple MRI Modalities Synthesis and Structural Segmentation of Mouse Brain, Ieee Transactions on Medical Imaging, 42 (2023) 1197-1209.
163. J. Jiang, Y.-C. Hu, N. Tyagi, P. Zhang, A. Rimner, G.S. Mageras, J.O. Deasy, H. Veeraraghavan, Tumor-aware, adversarial domain adaptation from CT to MRI for lung cancer segmentation, Medical Image Computing and Computer Assisted Intervention–MICCAI 2018: 21st International Conference, Granada, Spain, September 16-20, 2018, Proceedings, Part II 11, Springer, 2018, pp. 777-785.
164. C.B. Jin, H. Kim, W. Jung, S. Joo, E. Park, Y.S. Ahn, I.H. Han, J.I. Lee, X.N. Cui, CT-based MR Synthesis using Adversarial Cycle-consistent Networks with Paired Data Learning, 11th International Congress on Image and Signal Processing, BioMedical Engineering and Informatics (CISP-BMEI)Beijing, PEOPLES R CHINA, 2018.
165. X. Dong, Y. Lei, S. Tian, T. Wang, P. Patel, W.J. Curran, A.B. Jani, T. Liu, X. Yang, Synthetic MRI-aided multi-organ segmentation on male pelvic CT using cycle consistent deep attention network, Radiotherapy and Oncology, 141 (2019) 192-199.
166. H. Yang, K.J. Xia, A.Q. Bi, P.J. Qian, M.R. Khosravi, Ieee, Abdomen MRI synthesis based on conditional GAN, 6th Annual Conference on Computational Science and Computational Intelligence (CSCI)Las Vegas, NV, 2019, pp. 1021-1025.
167. X. Chen, C.F. Lian, L. Wang, H.N. Deng, S.H. Fung, D. Nie, K.H. Thung, P.T. Yap, J. Gateno, J.J. Xia, D.G. Shen, One-Shot Generative Adversarial Learning for MRI Segmentation of Craniomaxillofacial Bony Structures, Ieee Transactions on Medical Imaging, 39 (2020) 787-796.
168. L.M. Xu, X.H. Zeng, H. Zhang, W.S. Li, J.B. Lei, Z.W. Huang, BPGAN: Bidirectional CT-to-MRI prediction using multi-generative multi-adversarial nets with spectral normalization and localization, Neural Networks, 128 (2020) 82-96.
169. J.X. Chen, J. Wei, R. Li, TarGAN: Target-Aware Generative Adversarial Networks for Multi-modality Medical Image Translation, International Conference on Medical Image Computing and Computer Assisted Intervention (MICCAI)Electr Network, 2021, pp. 24-33.
170. Y. Lei, T.H. Wang, S.B. Tian, Y.B. Fu, P. Patel, A.B. Jani, W.J. Curran, T. Liu, X.F. Yang, Male pelvic CT multi-organ segmentation using synthetic MRI-aided dual pyramid networks, Physics in Medicine and Biology, 66 (2021).
171. R. Touati, W.T. Le, S. Kadoury, A feature invariant generative adversarial network for head and neck MRI/CT image synthesis, Physics in Medicine and Biology, 66 (2021).
172. H. Kang, A.R. Podgorsak, B.P. Venkatesulu, A.L. Saripalli, B. Chou, A.A. Solanki, M. Harkenrider, S. Shea, J.C. Roeske, M. Abuhamad, Prostate segmentation accuracy using synthetic MRI for high-dose-rate prostate brachytherapy treatment planning, Physics in Medicine and Biology, 68 (2023).
173. X. Han, MR-based synthetic CT generation using a deep convolutional neural network method, Medical physics, 44 (2017) 1408-1419.
174. H.F. Sun, Q.Y. Xi, J.W. Sun, R.B. Fan, K. Xie, X.Y. Ni, J.H. Yang, Research on new treatment mode of radiotherapy based on pseudo-medical images, Computer Methods and Programs in Biomedicine, 221 (2022).
175. C.H. Jiang, X. Zhang, N. Zhang, Q.Y. Zhang, C. Zhou, J.M. Yuan, Q. He, Y.F. Yang, X. Liu, H.R. Zheng, W. Fan, Z.L. Hu, D. Liang, Synthesizing PET/MR (T1-weighted) images from non-attenuation-corrected PET images, Physics in Medicine and Biology, 66 (2021).
176. J.B. Jiao, A.I.L. Namburete, A.T. Papageorghiou, J.A. Noble, Self-Supervised Ultrasound to MRI Fetal Brain Image Synthesis, Ieee Transactions on Medical Imaging, 39 (2020) 4413-4424.
177. A. Thummerer, B.A. de Jong, P. Zaffino, A. Meijers, G.G. Marmitt, J. Seco, R. Steenbakkers, J.A. Langendijk, S. Both, M.F. Spadea, A.C. Knopf, Comparison of the suitability of CBCT- and MR-based synthetic CTs for daily adaptive proton therapy in head and neck patients, Physics in Medicine and Biology, 65 (2020).

 doi:10.20944/preprints202512.1407.v1

178. T. Zhang, H. Pang, Y. Wu, J. Xu, Z. Liang, S. Xia, C. Jin, R. Chen, S.J.M. Qi, B. Engineering, Computing, InspirationOnly: synthesizing expiratory CT from inspiratory CT to estimate parametric response map, (2025) 1-18.
179. T. Zhang, H. Pang, Y. Wu, J. Xu, L. Liu, S. Li, S. Xia, R. Chen, Z. Liang, S.J.C.M. Qi, P.i. Biomedicine, BreathVisionNet: A pulmonary-function-guided CNN-transformer hybrid model for expiratory CT image synthesis, 259 (2025) 108516.
180. P. Yu, H. Zhang, D. Wang, R. Zhang, M. Deng, H. Yang, L. Wu, X. Liu, A.S. Oh, F.G.J.n.D.M. Abtin, Spatial resolution enhancement using deep learning improves chest disease diagnosis based on thick slice CT, 7 (2024) 335.
181. H.R. Yang, J. Sun, A. Carass, C. Zhao, J. Lee, J.L. Prince, Z.B. Xu, Unsupervised MR-to-CT Synthesis Using Structure-Constrained CycleGAN, Ieee Transactions on Medical Imaging, 39 (2020) 4249-4261.
182. R. Wei, B. Liu, F.G. Zhou, X.Z. Bai, D.S. Fu, B. Liang, Q.W. Wu, A patient-independent CT intensity matching method using conditional generative adversarial networks (cGAN) for single x-ray projection-based tumor localization, Physics in Medicine and Biology, 65 (2020).
183. Y.W. Zhang, C.P. Li, Z.H. Dai, L.M. Zhong, X.T. Wang, W. Yang, Breath-Hold CBCT-Guided CBCT-to-CT Synthesis via Multimodal Unsupervised Representation Disentanglement Learning, Ieee Transactions on Medical Imaging, 42 (2023) 2313-2324.
184. X. Dong, T.H. Wang, Y. Lei, K. Higgins, T. Liu, W.J. Curran, H. Mao, J.A. Nye, X.F. Yang, Synthetic CT generation from non-attenuation corrected PET images for whole-body PET imaging, Physics in Medicine and Biology, 64 (2019).
185. X.R. Zhou, W.W. Cai, J.J. Cai, F. Xiao, M.K. Qi, J.W. Liu, L.H. Zhou, Y.B. Li, T. Song, Multimodality MRI synchronous construction based deep learning framework for MRI-guided radiotherapy synthetic CT generation, Computers in Biology and Medicine, 162 (2023).
186. Y.H. Li, J.H. Zhu, Z.B. Liu, J.J. Teng, Q.Y. Xie, L.W. Zhang, X.W. Liu, J.P. Shi, L.X. Chen, A preliminary study of using a deep convolution neural network to generate synthesized CT images based on CBCT for adaptive radiotherapy of nasopharyngeal carcinoma, Physics in Medicine and Biology, 64 (2019).
187. X. Liang, L.Y. Chen, D. Nguyen, Z.G. Zhou, X.J. Gu, M. Yang, J. Wang, S. Jiang, Generating synthesized computed tomography (CT) from cone-beam computed tomography (CBCT) using CycleGAN for adaptive radiation therapy, Physics in Medicine and Biology, 64 (2019).
188. Y.G. Zhang, Y.R. Pei, H.F. Qin, Y.K. Guo, G.Y. Ma, T.M. Xu, H.B. Zha, Ieee, MASSETER MUSCLE SEGMENTATION FROM CONE-BEAM CT IMAGES USING GENERATIVE ADVERSARIAL NETWORK, 16th IEEE International Symposium on Biomedical Imaging (ISBI)Venice, ITALY, 2019, pp. 1188-1192.
189. A. Thummerer, P. Zaffino, A. Meijers, G.G. Marmitt, J. Seco, R. Steenbakkers, J.A. Langendijk, S. Both, M.F. Spadea, A.C. Knopf, Comparison of CBCT based synthetic CT methods suitable for proton dose calculations in adaptive proton therapy, Physics in Medicine and Biology, 65 (2020).
190. L.Y. Chen, X. Liang, C.Y. Shen, D. Nguyen, S. Jiang, J. Wang, Synthetic CT generation from CBCT images via unsupervised deep learning, Physics in Medicine and Biology, 66 (2021).
191. L.W. Deng, M.X. Zhang, J. Wang, S.J. Huang, X. Yang, Improving cone-beam CT quality using a cycle-residual connection with a dilated convolution-consistent generative adversarial network, Physics in Medicine and Biology, 67 (2022).
192. L.W. Deng, Y.F. Ji, S.J. Huang, X. Yang, J. Wang, Synthetic CT generation from CBCT using double-chain-CycleGAN, Computers in Biology and Medicine, 161 (2023).
193. J. Joseph, I. Biji, N. Babu, P.N. Pournami, P.B. Jayaraj, N. Puzhakkal, C. Sabu, V. Patel, Fan beam CT image synthesis from cone beam CT image using nested residual UNet based conditional generative adversarial network, Physical and Engineering Sciences in Medicine, 46 (2023) 703-717.
194. A. Szmul, S. Taylor, P. Lim, J. Cantwell, I. Moreira, Y. Zhang, D. D'Souza, S. Moinuddin, M.N. Gaze, J. Gains, C. Veiga, Deep learning based synthetic CT from cone beam CT generation for abdominal paediatric radiotherapy, Physics in Medicine and Biology, 68 (2023).
195. Z.L. Hu, Y.C. Li, S.J. Zou, H.Z. Xue, Z.R. Sang, X. Liu, Y.F. Yang, X.H. Zhu, D. Liang, H.R. Zheng, Obtaining PET/CT images from non-attenuation corrected PET images in a single PET system using Wasserstein generative adversarial networks, Physics in Medicine and Biology, 65 (2020).

 doi:10.20944/preprints202512.1407.v1

196. F. Rao, B. Yang, Y.W. Chen, J.S. Li, H.K. Wang, H.W. Ye, Y.F. Wang, K. Zhao, W.T. Zhu, A novel supervised learning method to generate CT images for attenuation correction in delayed pet scans, Computer Methods and Programs in Biomedicine, 197 (2020).
197. J.T. Li, Y.W. Wang, Y. Yang, X. Zhang, Z.J. Qu, S.B. Hu, Small animal PET to CT image synthesis based on conditional generation network, 14th International Congress on Image and Signal Processing, BioMedical Engineering and Informatics (CISP-BMEI)Shanghai, PEOPLES R CHINA, 2021.
198. X.D. Ying, H. Guo, K. Ma, J. Wu, Z.X. Weng, Y.F. Zheng, I.C. Soc, X2CT-GAN: Reconstructing CT from Biplanar X-Rays with Generative Adversarial Networks, 32nd IEEE/CVF Conference on Computer Vision and Pattern Recognition (CVPR)Long Beach, CA, 2019, pp. 10611-10620.
199. A. Lewis, E. Mahmoodi, Y.Y. Zhou, M. Coffee, E. Sizikova, I.C. Soc, Improving Tuberculosis (TB) Prediction using Synthetically Generated Computed Tomography (CT) Images, IEEE/CVF International Conference on Computer Vision (ICCVW)Electr Network, 2021, pp. 3258-3266.
200. G. Li, L. Bai, C.W. Zhu, E.H. Wu, R.B. Ma, A Novel Method of Synthetic CT Generation from MR Images based on Convolutional Neural Networks, 11th International Congress on Image and Signal Processing, BioMedical Engineering and Informatics (CISP-BMEI)Beijing, PEOPLES R CHINA, 2018.
201. M. Maspero, M.H.F. Savenije, A.M. Dinkla, P.R. Seevinck, M.P.W. Intven, I.M. Jurgenliemk-Schulz, L.G.W. Kerkmeijer, C.A.T. van den Berg, Dose evaluation of fast synthetic-CT generation using a generative adversarial network for general pelvis MR-only radiotherapy, Physics in Medicine and Biology, 63 (2018).
202. D. Nie, R. Trullo, J. Lian, L. Wang, C. Petitjean, S. Ruan, Q. Wang, D. Shen, Medical Image Synthesis with Deep Convolutional Adversarial Networks, Ieee Transactions on Biomedical Engineering, 65 (2018) 2720-2730.
203. L. Xiang, Q. Wang, D. Nie, L.C. Zhang, X.Y. Jin, Y. Qiao, D.G. Shen, Deep embedding convolutional neural network for synthesizing CT image from T1-Weighted MR image, Medical Image Analysis, 47 (2018) 31-44.
204. Y.H. Ge, D.M. Wei, Z. Xue, Q. Wang, X. Zhou, Y.Q. Zhan, S. Liao, Ieee, UNPAIRED MR TO CT SYNTHESIS WITH EXPLICIT STRUCTURAL CONSTRAINED ADVERSARIAL LEARNING, 16th IEEE International Symposium on Biomedical Imaging (ISBI)Venice, ITALY, 2019, pp. 1096-1099.
205. A. Largent, J.C. Nunes, H. Saint-Jalmes, J. Baxter, P. Greer, J. Dowling, R. de Crevoisier, O. Acosta, Ieee, PSEUDO-CT GENERATION FOR MRI-ONLY RADIOTHERAPY: COMPARATIVE STUDY BETWEEN A GENERATIVE ADVERSARIAL NETWORK, A U-NET NETWORK, A PATCH-BASED, AND AN ATLAS BASED METHODS, 16th IEEE International Symposium on Biomedical Imaging (ISBI)Venice, ITALY, 2019, pp. 1109-1113.
206. Y.Z. Liu, Y. Lei, Y.N. Wang, G. Shafai-Erfani, T.H. Wang, S.B. Tian, P. Patel, A.B. Jani, M. McDonald, W.J. Curran, T. Liu, J. Zhou, X.F. Yang, Evaluation of a deep learning-based pelvic synthetic CT generation technique for MRI-based prostate proton treatment planning, Physics in Medicine and Biology, 64 (2019).
207. Y.Z. Liu, Y. Lei, Y.N. Wang, T.H. Wang, L. Ren, L.Y. Lin, M. McDonald, W.J. Curran, T. Liu, J. Zhou, X.F. Yang, MRI-based treatment planning for proton radiotherapy: dosimetric validation of a deep learning-based liver synthetic CT generation method, Physics in Medicine and Biology, 64 (2019).
208. G. Zeng, G. Zheng, Hybrid generative adversarial networks for deep MR to CT synthesis using unpaired data, Medical Image Computing and Computer Assisted Intervention–MICCAI 2019: 22nd International Conference, Shenzhen, China, October 13–17, 2019, Proceedings, Part IV 22, Springer, 2019, pp. 759-767.
209. H. Arabi, G. Zeng, G. Zheng, H. Zaidi, Novel adversarial semantic structure deep learning for MRI-guided attenuation correction in brain PET/MRI, European journal of nuclear medicine and molecular imaging, 46 (2019) 2746-2759.
210. K. Boni, J. Klein, L. Vanquin, A. Wagner, T. Lacornerie, D. Pasquier, N. Reynaert, MR to CT synthesis with multicenter data in the pelvic area using a conditional generative adversarial network, Physics in Medicine and Biology, 65 (2020).
211. H. Emami, M. Dong, C.K. Glide-Hurst, I.C. Soc, Attention-Guided Generative Adversarial Network to Address Atypical Anatomy in Synthetic CT Generation, 21st IEEE International Conference on Information Reuse and Integration for Data Science (IEEE IRI)Electr Network, 2020, pp. 188-193.

 doi:10.20944/preprints202512.1407.v1

212. L. Fetty, T. Lofstedf, G. Heilemann, H. Furtado, N. Nesvacil, T. Nyholm, D. Georg, P. Kuess, Investigating conditional GAN performance with different generator architectures, an ensemble model, and different MR scanners for MR-sCT conversion, Physics in Medicine and Biology, 65 (2020).
213. L.L. Liu, A. Johansson, Y. Cao, J. Dow, T.S. Lawrence, J.M. Balter, Abdominal synthetic CT generation from MR Dixon images using a U-net trained with 'semi-synthetic' CT data, Physics in Medicine and Biology, 65 (2020).
214. H.A. Massa, J.M. Johnson, A.B. McMillan, Comparison of deep learning synthesis of synthetic CTs using clinical MRI inputs, Physics in Medicine and Biology, 65 (2020).
215. R. Oulbacha, S. Kadoury, Ieee, MRI TO CT SYNTHESIS OF THE LUMBAR SPINE FROM A PSEUDO-3D CYCLE GAN, IEEE 17th International Symposium on Biomedical Imaging (ISBI)Iowa, IA, 2020, pp. 1784-1787.
216. A. Abu-Srhan, I. Almallahi, M.A.M. Abushariah, W. Mahafza, O.S. Al-Kadi, Paired-unpaired Unsupervised Attention Guided GAN with transfer learning for bidirectional brain MR-CT synthesis, Computers in Biology and Medicine, 136 (2021).
217. M. Bajger, M.S. To, G. Lee, A. Wells, C. Chong, M. Agzarian, S. Poonnoose, Ieee, Lumbar Spine CT synthesis from MR images using CycleGAN - a preliminary study, International Conference on Digital Image Computing - Techniques and Applications (DICTA)Electr Network, 2021, pp. 420-427.
218. H. Chourak, A. Barateau, E. Mylona, C. Cadin, C. Lafond, P. Greer, J. Dowling, R. de Crevoisier, O. Acosta, Ieee, Voxel-Wise Analysis for Spatial Characterisation of Pseudo-CT Errors in MRI-Only Radiotherapy Planning, 18th IEEE International Symposium on Biomedical Imaging (ISBI)Nice, FRANCE, 2021, pp. 395-399.
219. H. Emami, M. Dong, S.P. Nejad-Davarani, C.K. Glide-Hurst, SA-GAN: Structure-Aware GAN for Organ-Preserving Synthetic CT Generation, International Conference on Medical Image Computing and Computer Assisted Intervention (MICCAI)Electr Network, 2021, pp. 471-481.
220. S.K. Kang, H.J. An, H. Jin, J.I. Kim, E.K. Chie, J.M. Park, J.S. Lee, Synthetic CT generation from weakly paired MR images using cycle-consistent GAN for MR-guided radiotherapy, Biomedical Engineering Letters, 11 (2021) 263-271.
221. R.R. Liu, Y. Lei, T.H. Wang, J. Zhou, J. Roper, L.Y. Lin, M.W. McDonald, J.D. Bradley, W.J. Curran, T. Liu, X.F. Yang, Synthetic dual-energy CT for MRI-only based proton therapy treatment planning using label-GAN, Physics in Medicine and Biology, 66 (2021).
222. Y.X. Liu, A.N. Chen, H.Y. Shi, S.J. Huang, W.J. Zheng, Z.Q. Liu, Q. Zhang, X. Yang, CT synthesis from MRI using multi-cycle GAN for head-and-neck radiation therapy, Computerized Medical Imaging and Graphics, 91 (2021).
223. S. Olberg, J. Chun, B.S. Choi, I. Park, H. Kim, T. Kim, J.S. Kim, O. Green, J.C. Park, Abdominal synthetic CT reconstruction with intensity projection prior for MRI-only adaptive radiotherapy, Physics in Medicine and Biology, 66 (2021).
224. R.Z. Wang, G.Y. Zheng, Ieee, DISENTANGLED REPRESENTATION LEARNING FOR DEEP MR TO CT SYNTHESIS USING UNPAIRED DATA, IEEE International Conference on Image Processing (ICIP)Electr Network, 2021, pp. 274-278.
225. S. Zenglin, P. Mettes, G. Zheng, C. Snoek, Frequency-Supervised MR-to-CT Image Synthesis, 1st Workshop on Deep Generative Models for Medical Image Computing and Computer Assisted Intervention (DGM4MICCAI) / 1st MICCAI Workshop on Data Augmentation, Labelling, and Imperfections (DALI)Electr Network, 2021, pp. 3-13.
226. S.P. Ang, S.L. Phung, M. Field, M.M. Schira, Ieee, AN IMPROVED DEEP LEARNING FRAMEWORK FOR MR-TO-CT IMAGE SYNTHESIS WITH A NEW HYBRID OBJECTIVE FUNCTION, 19th IEEE International Symposium on Biomedical Imaging (IEEE ISBI)Kolkata, INDIA, 2022.
227. G. Dovletov, D.D. Pham, S. Lörcks, J. Pauli, M. Gratz, H.H. Quick, Grad-CAM guided U-net for MRI-based pseudo-CT synthesis, 2022 44th Annual International Conference of the IEEE Engineering in Medicine & Biology Society (EMBC), IEEE, 2022, pp. 2071-2075.
228. G. Dovletov, D.D. Pham, J. Pauli, M. Gratz, H. Quick, Improved MRI-based Pseudo-CT Synthesis via Segmentation Guided Attention Networks, 15th International Joint Conference on Biomedical Engineering

 doi:10.20944/preprints202512.1407.v1

Systems and Technologies (BIOSTEC) / 9th International Conference on Bioimaging (BIOIMAGING)Electr Network, 2022, pp. 131-140.

229. P. Eshraghi Boroojeni, Y. Chen, P.K. Commean, C. Eldeniz, G.B. Skolnick, C. Merrill, K.B. Patel, H. An, Deep-learning synthesized pseudo-CT for MR high-resolution pediatric cranial bone imaging (MR-HiPCB), Magnetic resonance in medicine, 88 (2022) 2285-2297.
230. A.G. Hernandez, P. Fau, S. Rapacchi, J. Wojak, H. Mailleux, M. Benkreira, M. Adel, Generation of synthetic CT with Deep Learning for Magnetic Resonance Guided Radiotherapy, 16th International Conference on Signal-Image Technology and Internet-Based Systems (SITIS)Dijon, FRANCE, 2022, pp. 368-371.
231. A. Jabbarpour, S.R. Mahdavi, A.V. Sadr, G. Esmaili, I. Shiri, H. Zaidi, Unsupervised pseudo CT generation using heterogenous multicentric CT/MR images and CycleGAN: Dosimetric assessment for 3D conformal radiotherapy, Computers in Biology and Medicine, 143 (2022).
232. H. Liu, M.K. Sigona, T.J. Manuel, L.M. Chen, C.F. Caskey, B.M. Dawant, Synthetic CT Skull Generation for Transcranial MR Imaging-Guided Focused Ultrasound Interventions with Conditional Adversarial Networks, Conference on Medical Imaging - Image-Guided Procedures, Robotic Interventions, and ModelingElectr Network, 2022.
233. Q. Lyu, G. Wang, Conversion between ct and mri images using diffusion and score-matching models, arXiv preprint arXiv:2209.12104, (2022).
234. S.H. Park, D.M. Choi, I.H. Jung, K.W. Chang, M.J. Kim, H.H. Jung, J.W. Chang, H. Kim, W.S. Chang, Clinical application of deep learning-based synthetic CT from real MRI to improve dose planning accuracy in Gamma Knife radiosurgery: a proof of concept study, Biomedical Engineering Letters, 12 (2022) 359-367.
235. A. Ranjan, D. Lalwani, R. Misra, GAN for synthesizing CT from T2-weighted MRI data towards MR-guided radiation treatment, Magnetic Resonance Materials in Physics, Biology and Medicine, 35 (2022) 449-457.
236. H.F. Sun, Q.Y. Xi, R.B. Fan, J.W. Sun, K. Xie, X.Y. Ni, J.H. Yang, Synthesis of pseudo-CT images from pelvic MRI images based on an MD-CycleGAN model for radiotherapy, Physics in Medicine and Biology, 67 (2022).
237. S.I.Z. Estakhraji, A. Pirasteh, T. Bradshaw, A. McMillan, On the effect of training database size for MR-based synthetic CT generation in the head, Computerized Medical Imaging and Graphics, 107 (2023).
238. Y. Li, S.S. Xu, H.B. Chen, Y. Sun, J. Bian, S.S. Guo, Y. Lu, Z.Y. Qi, CT synthesis from multi-sequence MRI using adaptive fusion network, Computers in Biology and Medicine, 157 (2023).
239. X.M. Liu, J.L. Pan, X. Li, X.K. Wei, Z.P. Liu, Z.F. Pan, J.S. Tang, Attention Based Cross-Domain Synthesis and Segmentation From Unpaired Medical Images, Ieee Transactions on Emerging Topics in Computational Intelligence, (2023).
240. G. Parrella, A. Vai, A. Nakas, N. Garau, G. Meschini, F. Camagni, S. Molinelli, A. Barcellini, A. Pella, M. Ciocca, V. Vitolo, E. Orlandi, C. Paganelli, G. Baroni, Synthetic CT in Carbon Ion Radiotherapy of the Abdominal Site, Bioengineering-Basel, 10 (2023).
241. J.Y. Wang, Q.M.J. Wu, F. Pourpanah, An attentive-based generative model for medical image synthesis, International Journal of Machine Learning and Cybernetics, (2023).
242. L.F. Wang, Y. Liu, J. Mi, J. Zhang, MSE-Fusion: Weakly supervised medical image fusion with modal synthesis and enhancement, Engineering Applications of Artificial Intelligence, 119 (2023).
243. B. Zhao, T.T. Cheng, X.R. Zhang, J.J. Wang, H. Zhu, R.C. Zhao, D.W. Li, Z.J. Zhang, G. Yu, CT synthesis from MR in the pelvic area using Residual Transformer Conditional GAN, Computerized Medical Imaging and Graphics, 103 (2023).
244. T. Nyholm, S. Svensson, S. Andersson, J. Jonsson, M. Sohlin, C. Gustafsson, E. Kjellén, K. Söderström, P. Albertsson, L. Blomqvist, MR and CT data with multiobserver delineations of organs in the pelvic area—Part of the Gold Atlas project, Medical physics, 45 (2018) 1295-1300.
245. L.M. Zhong, Z.L. Chen, H. Shu, Y.K. Zheng, Y.W. Zhang, Y.K. Wu, Q.J. Feng, Y. Li, W. Yang, QACL: Quartet attention aware closed-loop learning for abdominal MR-to-CT synthesis via simultaneous registration, Medical Image Analysis, 83 (2023).
246. Y. Zhang, S. Miao, T. Mansi, R. Liao, Unsupervised X-ray image segmentation with task driven generative adversarial networks, Medical Image Analysis, 62 (2020).

 doi:10.20944/preprints202512.1407.v1

247. Y.X. Huang, F.X. Fan, C. Syben, P. Roser, L. Mill, A. Maier, Cephalogram synthesis and landmark detection in dental cone-beam CT systems, Medical Image Analysis, 70 (2021).
248. C. Peng, H.F. Liao, N. Wong, J.B. Luo, S.K. Zhou, R. Chellappa, I. Assoc Advancement Artificial, XraySyn: Realistic View Synthesis From a Single Radiograph Through CT Priors, 35th AAAI Conference on Artificial Intelligence / 33rd Conference on Innovative Applications of Artificial Intelligence / 11th Symposium on Educational Advances in Artificial IntelligenceElectr Network, 2021, pp. 436-444.
249. P.H.H. Yuen, X.H. Wang, Z.P. Lin, N.K.W. Chow, J. Cheng, C.H. Tan, W.M. Huang, CT2CXR: CT-based CXR Synthesis for Covid-19 Pneumonia Classification, 13th International Workshop on Machine Learning in Medical Imaging (MLMI)Singapore, SINGAPORE, 2022, pp. 210-219.
250. L.Y. Shen, L.Q. Yu, W. Zhao, J. Pauly, L. Xing, Novel-view X-ray projection synthesis through geometry-integrated deep learning, Medical Image Analysis, 77 (2022).
251. Y. Yan, H. Lee, E. Somer, V. Grau, Generation of Amyloid PET Images via Conditional Adversarial Training for Predicting Progression to Alzheimer's Disease, 1st International Workshop on PRedictive Intelligence in MEdicine (PRIME)Granada, SPAIN, 2018, pp. 26-33.
252. H. Emami, M. Dong, C. Glide-Hurst, CL-GAN: Contrastive Learning-Based Generative Adversarial Network for Modality Transfer with Limited Paired Data, European Conference on Computer Vision, Springer, 2022, pp. 527-542.
253. S.Y. Hu, B.Y. Lei, S.Q. Wang, Y. Wang, Z.G. Feng, Y.Y. Shen, Bidirectional Mapping Generative Adversarial Networks for Brain MR to PET Synthesis, Ieee Transactions on Medical Imaging, 41 (2022) 145-157.
254. J. Zhang, X.H. He, L.B. Qing, F. Gao, B. Wang, BPGAN: Brain PET synthesis from MRI using generative adversarial network for multi-modal Alzheimer's disease diagnosis, Computer Methods and Programs in Biomedicine, 217 (2022).
255. A. Ben-Cohen, E. Klang, S.P. Raskin, S. Soffer, S. Ben-Haim, E. Konen, M.M. Amitai, H. Greenspan, Cross-modality synthesis from CT to PET using FCN and GAN networks for improved automated lesion detection, Engineering Applications of Artificial Intelligence, 78 (2019) 186-194.
256. S. Olut, Y.H. Sahin, U. Demir, G. Unal, Generative Adversarial Training for MRA Image Synthesis Using Multi-contrast MRI, 1st International Workshop on PRedictive Intelligence in MEdicine (PRIME)Granada, SPAIN, 2018, pp. 147-154.
257. V.M. Campello, C. Martin-Isla, C. Izquierdo, S.E. Petersen, M.A.G. Ballester, K. Lekadir, Combining Multi-Sequence and Synthetic Images for Improved Segmentation of Late Gadolinium Enhancement Cardiac MRI, 10th International Workshop on Statistical Atlases and Computational Modelling of the Heart (STACOM)Shenzhen, PEOPLES R CHINA, 2019, pp. 290-299.
258. J.F. Zhao, D.W. Li, Z. Kassam, J. Howey, J. Chong, B. Chen, S. Li, Tripartite-GAN: Synthesizing liver contrast-enhanced MRI to improve tumor detection, Medical Image Analysis, 63 (2020).
259. A. Bone, S. Ammari, J.P. Lamarque, M. Elhaik, E. Chouzenoux, F. Nicolas, P. Robert, C. Balleyguier, N. Lassau, M.M. Rohe, Ieee, CONTRAST-ENHANCED BRAIN MRI SYNTHESIS WITH DEEP LEARNING: KEY INPUT MODALITIES AND ASYMPTOTIC PERFORMANCE, 18th IEEE International Symposium on Biomedical Imaging (ISBI)Nice, FRANCE, 2021, pp. 1159-1163.
260. M.Q. Pan, H. Zhang, Z.C. Tang, Y.H. Zhao, J. Tian, Ieee, Attention-Based Multi-Scale Generative Adversarial Network for synthesizing contrast-enhanced MRI, 43rd Annual International Conference of the IEEE-Engineering-in-Medicine-and-Biology-Society (IEEE EMBC)Electr Network, 2021, pp. 3650-3653.
261. C.C. Xu, D. Zhang, J. Chong, B. Chen, S. Li, Synthesis of gadolinium-enhanced liver tumors on nonenhanced liver MR images using pixel-level graph reinforcement learning, Medical Image Analysis, 69 (2021).
262. H.W. Chen, S.A. Yan, M.X. Xie, J.L. Huang, Application of cascaded GAN based on CT scan in the diagnosis of aortic dissection, Computer Methods and Programs in Biomedicine, 226 (2022).
263. T. Hu, M. Oda, Y. Hayashi, Z.Y. Lu, K.K. Kumamaru, T. Akashi, S. Aoki, K. Mori, Aorta-aware GAN for non-contrast to artery contrasted CT translation and its application to abdominal aortic aneurysm detection, International Journal of Computer Assisted Radiology and Surgery, 17 (2022) 97-105.
264. Y. Xue, B.E. Dewey, L.R. Zuo, S. Han, A. Carass, P.Y. Duan, S.W. Remedios, D.L. Pham, S. Saidha, P.A. Calabresi, J.L. Prince, Bi-directional Synthesis of Pre- and Post-contrast MRI via Guided Feature

 doi:10.20944/preprints202512.1407.v1

Disentanglement, 7th International Workshop on Simulation and Synthesis in Medical Imaging (SASHIMI)Singapore, SINGAPORE, 2022, pp. 55-65.

265. C. Chen, C. Raymond, W. Speier, X.Y. Jin, T.F. Cloughesy, D. Enzmann, B.M. Ellingson, C.W. Arnold, Synthesizing MR Image Contrast Enhancement Using 3D High-Resolution ConvNets, Ieee Transactions on Biomedical Engineering, 70 (2023) 401-412.
266. R.A. Khan, Y.G. Luo, F.X. Wu, Multi-level GAN based enhanced CT scans for liver cancer diagnosis, Biomedical Signal Processing and Control, 81 (2023).
267. A. Killekar, J. Kwiecinski, M. Kruk, C. Kepka, A. Shanbhag, D. Dey, P. Slomka, Pseudo-contrast cardiac CT angiography derived from non-contrast CT using conditional generative adversarial networks, Conference on Medical Imaging - Image ProcessingSan Diego, CA, 2023.
268. E. Kim, H.H. Cho, J. Kwon, Y.T. Oh, E.S. Ko, H. Park, Tumor-Attentive Segmentation-Guided GAN for Synthesizing Breast Contrast-Enhanced MRI Without Contrast Agents, Ieee Journal of Translational Engineering in Health and Medicine, 11 (2023) 32-43.
269. N.-C. Ristea, A.-I. Miron, O. Savencu, M.-I. Georgescu, N. Verga, F.S. Khan, R.T. Ionescu, CyTran: A Cycle-Consistent Transformer with Multi-Level Consistency for Non-Contrast to Contrast CT Translation, Neurocomputing, (2023).
270. S.H. Welland, G. Melendez-Corres, P.Y. Teng, H. Coy, A. Li, M.W. Wahi-Anwar, S. Raman, M.S. Brown, Using a GAN for CT contrast enhancement to improve CNN kidney segmentation accuracy, Conference on Medical Imaging - Image ProcessingSan Diego, CA, 2023.
271. H.X. Zhang, M.H. Zhang, Y. Gu, G.Z. Yang, Deep anatomy learning for lung airway and artery-vein modeling with contrast-enhanced CT synthesis, International Journal of Computer Assisted Radiology and Surgery, 18 (2023) 1287-1294.
272. L.M. Zhong, P.Y. Huang, H. Shu, Y. Li, Y.W. Zhang, Q.J. Feng, Y.K. Wu, W. Yang, United multi-task learning for abdominal contrast-enhanced CT synthesis through joint deformable registration, Computer Methods and Programs in Biomedicine, 231 (2023).
273. M.E.J.A.r.o.n. Raichle, Positron emission tomography, 6 (1983) 249-267.
274. J.E.J.C.c.m. Aldrich, Basic physics of ultrasound imaging, 35 (2007) S131-S137.
275. A. Grimwood, J. Ramalhinho, Z.M.C. Baum, N. Montana-Brown, G.J. Johnson, Y.P. Hu, M.J. Clarkson, S.P. Pereira, D.C. Barratt, E. Bonmati, Endoscopic Ultrasound Image Synthesis Using a Cycle-Consistent Adversarial Network, 2nd International Workshop on Advances in Simplifying Medical UltraSound (ASMUS)Electr Network, 2021, pp. 169-178.
276. R.J. Kim, E. Wu, A. Rafael, E.-L. Chen, M.A. Parker, O. Simonetti, F.J. Klocke, R.O. Bonow, R.M.J.N.E.J.o.M. Judd, The use of contrast-enhanced magnetic resonance imaging to identify reversible myocardial dysfunction, 343 (2000) 1445-1453.
277. R.R.J.R. Edelman, Contrast-enhanced MR imaging of the heart: overview of the literature, 232 (2004) 653-668.
278. C.A. Mallio, A. Radbruch, K. Deike-Hofmann, A.J. van der Molen, I.A. Dekkers, G. Zaharchuk, P.M. Parizel, B.B. Zobel, C.C.J.I.r. Quattrocchi, Artificial intelligence to reduce or eliminate the need for gadolinium-based contrast agents in brain and cardiac MRI: a literature review, 58 (2023) 746-753.
279. H. Alqahtani, M. Kavakli-Thorne, G. Kumar, Applications of generative adversarial networks (gans): An updated review, Archives of Computational Methods in Engineering, 28 (2021) 525-552.
280. J. Ho, A. Jain, P. Abbeel, Denoising diffusion probabilistic models, Advances in neural information processing systems, 33 (2020) 6840-6851.
281. F.-A. Croitoru, V. Hondru, R.T. Ionescu, M.J.I.T.o.P.A. Shah, M. Intelligence, Diffusion models in vision: A survey, (2023).
282. J. Song, C. Meng, S. Ermon, Denoising diffusion implicit models, arXiv preprint arXiv:2010.02502, (2020).
283. L. Yang, Z. Zhang, Y. Song, S. Hong, R. Xu, Y. Zhao, W. Zhang, B. Cui, M.-H.J.A.C.S. Yang, Diffusion models: A comprehensive survey of methods and applications, 56 (2023) 1-39.
284. B. Cao, H. Zhang, N. Wang, X. Gao, D. Shen, Auto-GAN: self-supervised collaborative learning for medical image synthesis, Proceedings of the AAAI conference on artificial intelligence, 2020, pp. 10486-10493.

 doi:10.20944/preprints202512.1407.v1

285. L. Sun, J. Wang, Y. Huang, X. Ding, H. Greenspan, J.J.I.j.o.b. Paisley, h. informatics, An adversarial learning approach to medical image synthesis for lesion detection, 24 (2020) 2303-2314.
286. M. Azadmanesh, B.S. Ghahfarokhi, M.A. Talouki, H.J.E.S.w.A. Eliasi, On the local convergence of GANs with differential Privacy: Gradient clipping and noise perturbation, 224 (2023) 120006.
287. G. Hinton, O. Vinyals, J.J.a.p.a. Dean, Distilling the knowledge in a neural network, (2015).
288. T. Miyato, T. Kataoka, M. Koyama, Y.J.a.p.a. Yoshida, Spectral normalization for generative adversarial networks, (2018).
289. C. Kim, S. Park, H.J.J.I.T.o.N.N. Hwang, L. Systems, Local stability of wasserstein GANs with abstract gradient penalty, 33 (2021) 4527-4537.
290. J. Yim, D. Joo, J. Bae, J. Kim, A gift from knowledge distillation: Fast optimization, network minimization and transfer learning, Proceedings of the IEEE conference on computer vision and pattern recognition, 2017, pp. 4133-4141.
291. X. Wang, K. Yu, S. Wu, J. Gu, Y. Liu, C. Dong, Y. Qiao, C. Change Loy, Esrgan: Enhanced super-resolution generative adversarial networks, Proceedings of the European conference on computer vision (ECCV) workshops, 2018, pp. 0-0.
292. T. Salimans, I. Goodfellow, W. Zaremba, V. Cheung, A. Radford, X.J.A.i.n.i.p.s. Chen, Improved techniques for training gans, 29 (2016).
293. T.-C. Wang, M.-Y. Liu, J.-Y. Zhu, A. Tao, J. Kautz, B. Catanzaro, High-resolution image synthesis and semantic manipulation with conditional gans, Proceedings of the IEEE conference on computer vision and pattern recognition, 2018, pp. 8798-8807.